https://doi.org/10.5194/egusphere-2025-3190
Preprint. Discussion started: 23 July 2025

Annual and seasonal CO_2 flux in a temperate north-Patagonian peatland exposed to varying intensities of commercial *Sphagnum* moss harvesting

Patricio A. Pacheco-Cancino[1,2], Rubén F. Carrillo-López[1], Jorge A. Riquelme-Belmar[1], Marcelo A. Somos-Valenzuela[3]

[1] Department of Agronomic Sciences and Natural Resources, Faculty of Agricultural and Environmental Sciences, Universidad de La Frontera, Temuco, Chile.

[2] Ph.D. Program in Agri-Food and Environmental Sciences, Faculty of Agricultural and Environmental Sciences, Universidad de La Frontera, Temuco, Chile.

[3] Department of Forest Sciences, Faculty of Agricultural and Environmental Sciences, Universidad de La Frontera, Temuco, Chile

***Corresponding author**

Patricio Pacheco-Cancino.

Phone: +56 45 2596527

E-mail: patricio.pacheco@ufrontera.cl

https://doi.org/10.5194/egusphere-2025-3190
Preprint. Discussion started: 23 July 2025

Abstract

Peatlands hold the largest carbon (C) reserves worldwide and therefore play a fundamental role in climate change mitigation. In the Southern Hemisphere, peatlands distributed in the Patagonia represent the principal extratropical C sink. Nevertheless, increasing anthropogenic pressures, such as the commercial harvesting of *Sphagnum* moss, threaten their capacity to regulate CO_2 fluxes, a situation that has been scarcely studied.

We conducted a field study that quantified and analyzed the annual and seasonal CO_2 fluxes in a North Patagonian peatland subjected to varying intensities of commercial *Sphagnum* harvesting: high, moderate, and undisturbed. Using closed chamber techniques, we measured the components of the CO_2 flux over the course of one year, while also identifying the predominant environmental drivers influencing these fluxes.

The results showed that moss harvesting intensity was directly correlated with net ecosystem exchange (NEE) fluxes. The high-intensity extraction site acted as a net CO_2 source (375.7 g CO_2-C m^{-2} yr^{-1}), the moderately harvested site was approximately carbon neutral (10.2 g CO_2-C m^{-2} yr^{-1}), and the undisturbed site functioned as an annual CO_2 sink (−167.1 g CO_2-C m^{-2} yr^{-1}). Seasonal fluxes revealed that disturbed sites emitted more CO_2 in summer and acted as sinks in spring, while the undisturbed site sequestered CO_2 year-round. In winter, all three sites functioned as CO_2 sinks due to environmental conditions that favored productivity and minimized respiration.

Photosynthetically active radiation was the key bioclimatic driver regulating gross primary production and NEE, while air and soil temperature primarily influenced ecosystem respiration. These findings provide relevant evidence for understanding carbon dynamics in peatlands affected by commercial *Sphagnum* harvesting and underscore the need for sustainable management regulations to preserve their role as carbon sinks in Chilean Patagonia.

https://doi.org/10.5194/egusphere-2025-3190
Preprint. Discussion started: 23 July 2025

1. Introduction

Peatlands are ecosystems that develop under conditions of water saturation and low oxygen availability in the soil (Finlayson & Milton, 2016; Dickopp et al., 2018). They play a crucial role in climate change mitigation due to their capacity to store large amounts of carbon (C) in the form of partially decomposed organic matter (Blodau, 2002; Yu, 2012; Harenda et al., 2018; Strack et al., 2022; Li et al., 2024). This carbon storage is essential for understanding global biogeochemical processes, as peatlands hold approximately 30% of the Earth's terrestrial carbon, equivalent to twice the carbon stored in forest biomass, despite covering only 3% of the global land surface (Limpens et al., 2008; Yu et al., 2010; Joosten et al., 2016; Leifeld & Menichetti, 2018; Leifeld et al., 2019).

Throughout the Holocene, peatlands have acted as carbon sinks by capturing atmospheric CO_2 that would otherwise contribute to rising concentrations of this greenhouse gas in the Earth's atmosphere (Dunn & Freeman, 2011; Sirin, 2022; Helbig et al., 2022; Strack et al., 2022). However, their fragility and vulnerability to anthropogenic disturbances pose a significant risk to global climate stability (Frolking et al., 2011; Harris et al., 2022; Loisel & Gallego-Sala, 2022). The release of stored carbon due to peatland degradation represents a major source of CO_2 emissions, potentially undermining efforts to mitigate climate change (Loisel et al., 2021; Strack et al., 2022; UNEP, 2022; Mattila, 2024).

The anthropogenic pressures exerted on peatlands differ markedly between the Northern and Southern Hemispheres in terms of timing, intensity and type of disturbance. In this regard, Southern Hemisphere peatlands have been less affected by direct human impacts and degradation processes (León et al., 2021; UNEP, 2022). Nonetheless, temperate peatlands in the Southern Hemisphere, particularly those distributed across Australasia and Patagonia, have increasingly been subjected to anthropogenic pressures, mainly related to peat and *Sphagnum* moss extraction (Whinam & Buxton, 1997; Whinam et al., 2003; León et al., 2021; Lopatin et al., 2022; Pacheco-Cancino et al., 2025).

https://doi.org/10.5194/egusphere-2025-3190
Preprint. Discussion started: 23 July 2025

Temperate peatlands located in the northern region of Chilean Patagonia (41°–45° S) have shown a sustained increase in *Sphagnum* moss harvesting in recent decades, driven by strong commercial interest and growing international demand, especially from Asian markets (Díaz et al., 2012; Díaz & Silva, 2018; Blok et al., 2021). As a result, many peatlands in this region exhibit signs of unsustainable moss harvesting, posing a threat to their ecological stability and functionality (León et al., 2012; Díaz & Silva, 2018). Despite this, there is a notable lack of scientific evidence addressing the impacts of this disturbance on the ecosystem services provided by these environments, particularly concerning CO_2 fluxes. This gap is especially concerning given that Patagonian peatlands represent the primary extratropical carbon sink and reservoir in the Southern Hemisphere (UNEP, 2022; Pérez-Quezada et al., 2023).

Recent studies suggest that disturbances associated with *Sphagnum* moss harvesting can significantly alter the processes of CO_2 capture and release in peatlands (Silvan et al., 2017; Valdés-Barrera et al., 2019; Karjalainen et al., 2025). However, few studies have examined how varying intensities of commercial *Sphagnum* extraction influence annual and seasonal CO_2 flux dynamics, as most analyses are limited to the vegetation growing season. Expanding the temporal scope of such studies is essential to better understand flux dynamics and develop strategies for the conservation and sustainable management of these ecosystems and their associated resources.

To address this knowledge gap, we performed in situ measurements of CO_2 flux components using transparent and opaque closed chambers over the course of one year, including the seasonal dynamics, in two sites subjected to different commercial extraction intensities of *Sphagnum magellanicum* and one undisturbed site, located in a temperate peatland in northern Chilean Patagonia. In addition, we identified the environmental drivers that most strongly influenced CO_2 fluxes at each study site. We hypothesized that increasing *Sphagnum* harvesting intensity would lead to greater annual and seasonal CO_2 emissions to the atmosphere. The specific objectives of this study were: i) to quantify annual and seasonal CO_2 fluxes at two sites under different levels of *Sphagnum* moss harvesting and one undisturbed site in a North Patagonian peatland, ii) to analyze and compare the components of annual and seasonal CO_2 fluxes among

https://doi.org/10.5194/egusphere-2025-3190
Preprint. Discussion started: 23 July 2025

sites with varying harvesting intensities and an undisturbed area, and iii) to identify the main environmental drivers influencing annual CO_2 fluxes at the different study sites.

2. Materials and methods

2.1. Study area

The study area is located in the province of Llanquihue, Los Lagos Region, approximately 28 km east of the city of Puerto Montt (41°34'S, 72°42'W) (Fig. 1, Pacheco-Cancino et al. (2025)). It corresponds to a transitional minerotrophic peatland formed as a result of human activity associated with forest fires and intensive logging of native forests (Díaz et al., 2008; León et al., 2018), developed on volcanic ash-derived soils locally known as *"ñadis"*. These soils feature a placic horizon, which leads to poor drainage and waterlogging, particularly during the winter season (Carrasco et al., 2017). The climate in the area is classified as temperate rainy with oceanic influence (Di Castri & Hajek, 1976), with a 30-year mean annual temperature of 10.3° C and an average annual precipitation of 1560 mm (reference period 1991–2020, Chilean Weather Service). The average depth of the peat layer in the study area is 0.66 m.

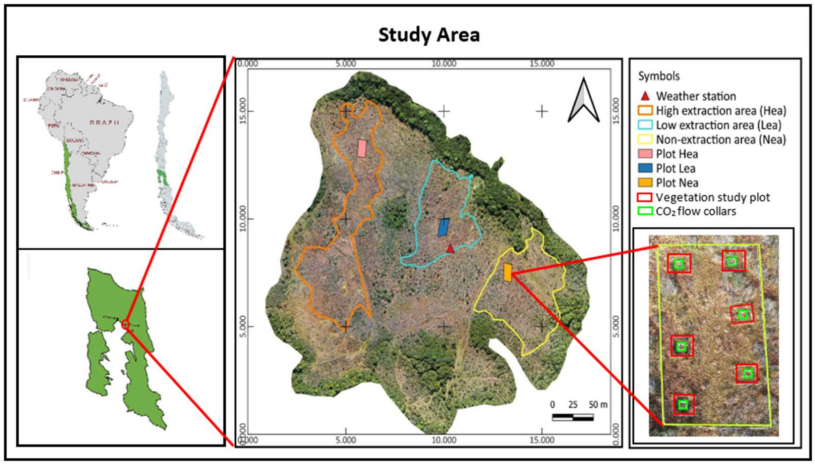

Figure 1. Location of the study area, sites with different intensities of commercial *Sphagnum* moss harvesting, and undisturbed site; sampling areas within each site and distribution of point measurement units for CO_2 fluxes. Obtained from Pacheco-Cancino *et al.* (2025).

https://doi.org/10.5194/egusphere-2025-3190
Preprint. Discussion started: 23 July 2025

Two distinct areas with differing intensities of *Sphagnum* moss harvesting were identified within the study site. The first area covers approximately 1 ha and has been harvested using tools (hooks and forks) during successive seasons over the past eight years, following a high-intensity extraction scheme (H-ea). In the most recent moss harvesting season prior to the study, an area of approximately 850 m² was disturbed, leaving heterogeneously distributed undisturbed patches with a residual moss cover of less than 30%. The microtopography in H-ea is characterized by a predominance of lawns, along with fewer hollows and minor hummocks. The main vegetation species present at this site include *Sphagnum magellanicum* Brid., *Sphagnum fimbriatum* Wilson, *Juncus procerus* E. Mey., *Juncus stipulatus* Nees & Meyen, *Gaultheria pumila* (L.f.) D.J. Middleton, and *Myrteola nummularia* (Poir.) O. Berg. Among vascular plants, small shrub species represent the dominant functional group in terms of surface cover. The second area encompasses approximately 0.5 ha and, unlike H-ea, moss harvesting has been carried out manually under a less intensive extraction scheme (L-ea). In the most recent extraction period prior to the study, a ~350 m² section was disturbed, maintaining a residual moss cover of around 50%. The microtopography in L-ea features low hummocks, lawns, and some marginal hollows. The main vegetation species in this site include those already described for H-ea, along with *Gaultheria antarctica* Hook.f., *Rubus geoides* Sm., *Carex magellanica* Lam., *Ugni molinae* Turcz., *Empetrum rubrum* Vahl ex Willd., and *Eucryphia cordifolia* Cav. In this case, among vascular plants, herbaceous species represent the group with the greatest coverage. Additionally, a third undisturbed site of approximately 0.8 ha with 100% *Sphagnum* moss cover (N-ea) was included as a reference area. This site exhibits irregular microtopography composed of taller hummocks than those observed in L-ea, along with lawn zones. In addition to the species already described for the previous two sites, the vegetation at this location includes *Gaultheria mucronata* (L.f.) Hook. & Arn., *Baccharis concava* (Ruiz & Pav.) Pers., *Tepualia stipularis* (Hook. & Arn.) Griseb., *Amomyrtus meli* (Phil.) D. Legrand & Kausel, *Amomyrtus luma* (Molina) D. Legrand & Kausel, *Caldcluvia paniculata* (Cav.) D. Don, *Weinmannia trichosperma* Cav., and *Drimys winteri* J.R. Forst. & G. Forst. In this case, tree species exhibit the highest coverage among vascular plants.

https://doi.org/10.5194/egusphere-2025-3190
Preprint. Discussion started: 23 July 2025

2.2. CO_2 flux measurements

At each study site, a 200 m² plot (20 × 10 m) was delineated, within which six sampling units (SUs) were randomly established for conducting point-based CO_2 flux measurements (Fig. 1). The SUs were located in representative areas reflecting the conditions of the moss harvesting sites and the reference site, maintaining a minimum distance of 2 m between the edges of each SU and the margins of the 200 m² plot. A total of 18 SUs were established across the study area.

We conducted CO_2 flux measurements on two consecutive days approximately every 15 days during the vegetation growing season, between 20 November 2021, and 14 April 2022. Outside of the growing season, that is, between 15 April and 19 November 2022, measurements were carried out once or twice per month, with reduced sampling intensity due to lower net CO_2 exchange between the ecosystem and the atmosphere (Alm et al., 1999; Saarnio et al., 2007). This schedule resulted in a total of 32 field sampling dates over the course of the study period. Eighteen PVC collars (six per plot at each site), measuring 60 × 60 cm, were permanently installed to a depth of ~20 cm at the center of each SU (Fig. 1), which could be accessed by installing boardwalks to avoid soil disturbances. Each collar had an upper groove that allowed for the placement of a plexiglass closed chamber (60 × 60 × 50 cm, 95% transparency) used to record CO_2 fluxes (Heinemeyer & McNamara, 2011; Pavelka et al., 2018). The groove also enabled an airtight water seal during measurement. To measure CO_2 fluxes, a custom-built device was installed in the chamber headspace. The system was based on an Arduino™ microcontroller and included a non-dispersive infrared CO_2 sensor (model 030–8-0010 K30 FR, SenseAir, Sweden) and a barometric pressure sensor (model BMP-280, Bosch, Germany), similar to the setup described by Mecagga et al. (2024). The device was developed by the Department of Electronic Engineering at Universidad de La Frontera. The K30 FR sensor was selected for its proven accuracy and reliability in CO_2 flux studies in peatlands (Mecagga et al., 2024; Martin et al., 2017). Calibration was performed using GasLab® 2.3.1.4 software by comparing CO_2 fluxes recorded with the K30 FR to those from an EGM-4 IRGA (PP-Systems), with adjustments for temperature, pressure, and relative humidity (Martin et al., 2017).

https://doi.org/10.5194/egusphere-2025-3190
Preprint. Discussion started: 23 July 2025

The chamber was also equipped with an air temperature and humidity sensor (Hobo U23 Pro v2, USA) and two small fans (Sunon, MagLev, Taiwan) to ensure adequate air mixing inside the chamber headspace. A vent tube was installed to equalize pressure during chamber placement and removal. Net ecosystem exchange (NEE) was measured during daytime under full sunlight with the transparent chamber installed for five minutes, recording CO_2 concentrations at one second intervals. Subsequently, the chamber was covered with a reflective, insulating hood to simulate dark conditions and measure ecosystem respiration (R_{eco}), which includes both autotrophic (R_a) and heterotrophic (R_h) respiration. R_{eco} measurements were conducted at similar intervals and durations as those for NEE. Gross primary production (GPP) was calculated as the difference between NEE and R_{eco}, following the expression proposed by Samaritani et al. (2011), Beetz et al. (2013), and Eickenscheidt et al. (2015):

$$NEE = GPP + R_{eco} \quad (1)$$

Between each measurement, the chamber was ventilated by gently shaking it to restore ambient CO_2 concentration. Two complete measurement cycles were conducted per extraction area and sampling day: one between 9:00 and 13:00 h, and another between 14:00 and 18:00 h during the growing season; and from 8:30 to 12:30 h and 13:00 to 17:00 h during the non-growing season. This schedule aimed to capture the diurnal variation in environmental conditions. CO_2 flux rates were calculated based on the linear change in CO_2 concentration over time (Brown et al., 2017; Pavelka et al., 2018; Laine et al., 2019), considering the chamber volume, surface area, internal temperature, and atmospheric pressure, in accordance with the ideal gas law (Wright et al., 2011; Järveoja et al., 2018). Fluxes were derived by fitting a linear regression, following methods described in previous studies (Riutta et al., 2007; Juszczak et al., 2012; Murray et al., 2017; D'Angelo et al., 2021). Only measurements with regression R^2 values ≥ 0.90 were considered. The atmospheric sign convention was used to interpret CO_2 exchange, whereby positive fluxes indicate net CO_2 emissions from the ecosystem, and negative fluxes represent net CO_2 uptake by the ecosystem (Elsgaard et al., 2012; Järveoja et al., 2018).

https://doi.org/10.5194/egusphere-2025-3190
Preprint. Discussion started: 23 July 2025

2.3. Environmental variable data recording

During CO_2 flux measurements at each site, we recorded environmental variables considered relevant for evaluating their relationship (positive, negative, or neutral) with the components of annual and seasonal CO_2 fluxes (GPP, R_{eco}, and NEE). In this context, the water table level (WT) was measured using perforated PVC piezometers (1 m depth, 75 mm diameter), with holes every 10 cm, installed 0.5 m from the edges of each sampling unit. WT depth was recorded using a pressure transducer (Keller model DCX-22, Switzerland). Additionally, during each chamber installation, the following variables were recorded: incident photosynthetically active radiation (PAR) using a quantum sensor (Apogee model MQ-200, Utah, USA); soil temperature and volumetric moisture content at depths of 5 and 10 cm (ST_5, ST_{10}, SMC_5, SMC_{10}) using a stainless-steel probe (RK520–01 sensor, Rika Electronics Tech, China); and air temperature and relative humidity outside the chamber using a thermohygrometer (Extech model 444703, Taiwan).

An automated weather station (model UC-NCR-VIA-10-S100-HOBO U30, USA) was installed in the study area to continuously record various environmental variables. The weather station was placed 30 m south of the L-ea site and was programmed to record data every 30 minutes for the following variables: air temperature (T_{air}), relative humidity (RH), precipitation (Pp), solar radiation (SR), atmospheric pressure (AP), photosynthetically active radiation, water table level, and soil temperature and moisture at depths of 5 and 10 cm.

2.4. Modelling of CO_2 flux components (GPP, R_{eco}, and NEE)

Ecosystem respiration in peatlands is primarily influenced by air and soil temperature (Updegraff et al., 2001; Lafleur et al., 2005; Juszczak et al., 2013; Swails et al., 2022; Rankin et al., 2023). Therefore, R_{eco} is commonly modeled as an exponential or polynomial function of temperature (Kelly et al., 2021; Swails et al., 2022). In this context, Lloyd & Taylor (1994) proposed that the relationship between R_{eco} and temperature can be accurately described by an Arrhenius type equation, in which the effective activation energy for respiration varies inversely with temperature. The exponential regression model suggested by

https://doi.org/10.5194/egusphere-2025-3190
Preprint. Discussion started: 23 July 2025

Lloyd and Taylor (1994) has demonstrated high reliability in various studies assessing CO_2 fluxes in different types of peatlands (Elsgaard et al., 2012; Beetz et al., 2013; Eickenscheidt et al., 2015; D'Angelo et al., 2021), and was selected in this study to model R_{eco}:

$$R_{eco} = R_{ref} \times exp\left[E_0 \left(\frac{1}{T_{ref}-T_0} - \frac{1}{T_{soil}-T_0}\right)\right] \quad (2)$$

Where R_{eco} is the measured ecosystem respiration rate, R_{ref} is respiration at the reference temperature, E_o is the activation energy (K), T_{ref} is the reference temperature (283.15 K), T_o is the constant baseline temperature for the onset of biological processes (227.13 K), and T_{soil} is the best fit temperature variable among those recorded in the study, i.e., T_{air}, ST_5, or ST_{10}.

R_{ref} and E_o were calculated using field measured R_{eco} data through the Microsoft Excel® Solver add-in (Beyer & Höper, 2015; Baird et al., 2019). In this case, the objective function was to minimize model error (Eq. 2), obtained by summing the squared differences between observed and modeled R_{eco} values (Baird et al., 2019). The selected R_{ref} and E_o values were those generated by a model adjusted according to the temperature variable (T_{air}, ST_5, or ST_{10}) that produced the highest coefficient of determination (R^2) from a linear regression between modeled and observed data. Linear interpolation was used to estimate R_{ref} and E_o values between successive field campaigns. R_{eco} fluxes were then calculated at 30-minute intervals using temperature data recorded by the weather station (Beyer & Höper, 2015; Eickenscheidt et al., 2015), which allowed the calculation of daily, seasonal, and annual R_{eco} fluxes.

On the other hand, light availability, expressed as irradiance (PAR), plays a crucial role in estimating GPP in peatlands, due to its influence on species specific photosynthetic rates under non-limiting light conditions (Peichl et al., 2018). In general, the relationship between PAR and GPP can be described by a rectangular hyperbolic function of the Michaelis-Menten type (Michaelis & Menten, 1913; Johnson & Godoy, 2011; Laine et al., 2016). Therefore, this approach was adopted in the present study, given its

https://doi.org/10.5194/egusphere-2025-3190
Preprint. Discussion started: 23 July 2025

widespread use in research on various types of peatlands (Baird et al., 2019). The model used was the following:

$$GPP = \frac{GPP_{max}\ x\ \alpha\ x\ PAR}{GPP_{max} + \alpha\ x\ PAR} \quad (3)$$

Where *PAR* is the photon flux density of photosynthetically active radiation, α is the initial slope of the regression curve associated with light use efficiency, and GPP_{max} is the upper limit of production rate as PAR approaches infinity (Beetz et al., 2013).

The same methodological approach used to determine R_{eco} model parameters was applied here, using the Excel Solver add in to estimate α and GPP_{max}. Values for both parameters between successive field campaigns were obtained through linear interpolation. Daily, seasonal, and annual accumulated GPP fluxes were calculated from the modeled α and GPP_{max} values in combination with the PAR records stored by the weather station at 30-minute intervals. To account for the reflection and absorption of incoming radiation by the transparent chamber, PAR values were reduced by 5% for GPP modeling, following Eickenscheidt et al. (2015).

Additionally, seasonal NEE records were reconstructed at 30-minute intervals for each study site using Eq. (1). In this calculation, modeled GPP values were treated as negative (indicating CO_2 uptake), while R_{eco} values were treated as positive (representing CO_2 release to the atmosphere), in accordance with the atmospheric sign convention (Baird et al., 2019).

2.5. Statistical analyses

Data for the CO_2 flux components obtained from the sampling units (SUs) at each site were averaged to avoid pseudoreplication (Järveoja et al., 2016; Peichl et al., 2018). Consequently, site level means were calculated by averaging the values from the six SUs per site (Swails et al., 2022). The normality of GPP, R_{eco}, and NEE datasets was assessed with the Kolmogorov–Smirnov test; because the data deviated from

https://doi.org/10.5194/egusphere-2025-3190
Preprint. Discussion started: 23 July 2025

normality, non-parametric tests were applied. We used the Kruskal–Wallis analysis of variance (ANOVA) followed by Dunn's multiple comparison test with Bonferroni correction to evaluate the significance of differences in CO_2 fluxes (GPP, R_{eco}, and NEE) among sites (Heinemeyer et al., 2018; Viru et al., 2020; Swails et al., 2022). In all cases, *p*-values < 0.05 were considered statistically significant. To identify the main environmental drivers of CO_2 fluxes, we performed partial least squares regression (PLS-R) analysis (Bayer et al., 2012; Peichl et al., 2014). PLS-R transforms predictor variables into orthogonal components, providing a solution to multicollinearity in multiple linear regression and reducing data dimensionality (Vega-Vilca & Guzmán, 2011). This method was selected because several environmental variables were highly correlated. It reduced the set of predictors to a smaller number of uncorrelated principal components, thereby preventing instability in regression coefficients. The PLS-R analyses used the nonlinear iterative partial least squares (NIPALS) algorithm, Jackknife cross validation, and variable importance in projection (VIP) scores to evaluate the influence of each environmental factor. All statistical analyses were carried out with XLSTAT software.

3. Results

3.1. Meteorological conditions

Total precipitation recorded during the study period was 1250 mm, representing a 20.2% deficit compared to the 30-year historical annual average (1567 mm; 1991–2020). The months with the greatest rainfall deficits relative to the historical average were December, August, and May, with deficits of 57%, 47%, and 46%, respectively. Conversely, the months with the highest surplus compared to historical values were July and February, with surpluses of 15% and 6%, respectively. During the study period, the highest monthly precipitation was recorded in June and July, with 172 mm and 204 mm, respectively. The driest months were November and December, with 67 mm and 40 mm, respectively (Fig. 2). The average air temperature during the study period was 10.1 °C, which was 0.4 °C lower than the 30-year historical mean (1991–2020). However, the months of November, December, January, and February recorded monthly

https://doi.org/10.5194/egusphere-2025-3190
Preprint. Discussion started: 23 July 2025

mean temperatures above historical averages. In contrast, May and June exhibited the lowest deviations below the historical mean (Fig. 2). The highest monthly mean air temperature was observed in January (14.9 °C), and the lowest in June (5.2 °C).

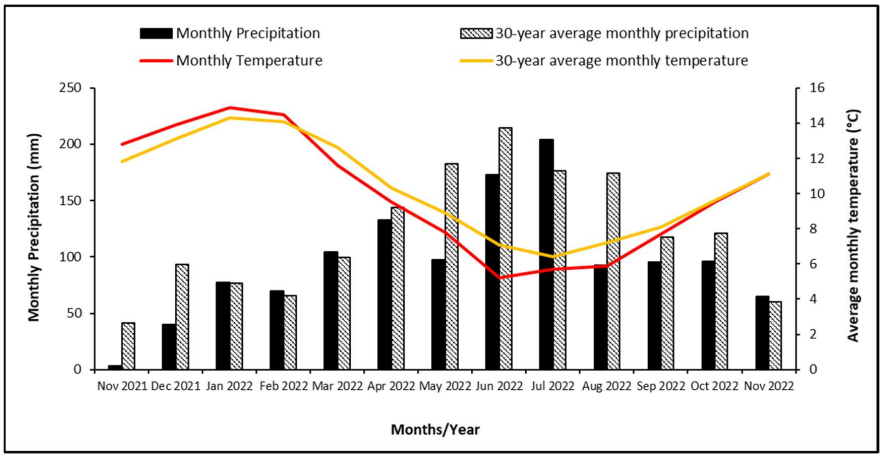

Figure 2. Records of monthly total precipitation and monthly mean temperature during the study period, and their comparison with 30-year historical records (1991–2020).

3.2. Annual behavior of environmental variables

Annual analysis of SMC_5 revealed significant differences among the three sites ($H = 213.9$; $p < 0.0001$), with H-ea recording the highest values and N-ea the lowest. Dunn's pairwise multiple comparison test also indicated statistically significant differences among all sites ($p < 0.0001$). The annual mean SMC_5 across the sites was 0.389 ± 0.066, 0.340 ± 0.047, and 0.320 ± 0.037 $m^3\ m^{-3}$ for H-ea, L-ea, and N-ea, respectively (Fig. S1). Seasonal analysis also showed significant differences among sites within each season (summer: $H = 151.1$; $p < 0.0001$; autumn: $H = 93.7$; $p < 0.0001$; winter: $H = 196.6$; $p < 0.0001$; spring: $H = 60.2$; $p < 0.0001$). Annual analysis of SMC_{10} also exhibited significant differences among sites ($H = 38.2$; $p < 0.0001$), although pairwise comparisons indicated significant differences only between N-ea and the other two sites ($p < 0.0001$). The annual mean SMC_{10} values were 0.390 ± 0.036, 0.386 ± 0.036, and 0.402 ± 0.048 $m^3\ m^{-3}$ for H-ea, L-ea, and N-ea, respectively (Fig. S2). At the seasonal level, SMC_{10} differed significantly among sites

https://doi.org/10.5194/egusphere-2025-3190
Preprint. Discussion started: 23 July 2025

in autumn (H = 22.1; p < 0.0001), winter (H = 52.1; p < 0.0001), and spring (H = 15.6; p < 0.0001), but not in summer (H = 3.9; p = 0.14). Both variables exhibited annual peaks in early July 2022, due to elevated cumulative rainfall over the preceding two days (53.6 mm), and the lowest values in late November, associated with low precipitation during the first 23 days of the month (41 mm). All three study sites recorded the highest seasonal averages of SMC_5 and SMC_{10} in winter and the lowest in summer (Table 1).

Table 1. Mean, minimum, and maximum values of seasonal daily average records of environmental variables for each study site.

Sites	Environmental Variables	Summer			Autumn			Winter			Spring		
		Min	Max	$\bar{X}$	Min	Max	$\bar{X}$	Min	Max	$\bar{X}$	Min	Max	$\bar{X}$
H-ea	SMC_5 (m^3/m^3)	0.290	0.365	0.325	0.318	0.545	0.392	0.410	0.541	0.455	0.265	0.487	0.361
	SMC_{10} (m^3/m^3)	0.326	0.396	0.359	0.359	0.533	0.403	0.385	0.572	0.418	0.302	0.425	0.366
	ST_5 (°C)	16.2	24.5	20.6	4.8	19.1	13.4	5.5	16.2	13.4	10.7	22.1	17.1
	ST_{10} (°C)	15.2	21.6	18.6	6.5	17.4	13.2	6.7	16.3	11.7	11.8	19.6	15.9
	WT (cm)	-2.6	-20.6	-14.4	1.7	-13.3	-7.4	2.4	-13.4	-6.1	-0.8	-20.1	-10.9
L-ea	SMC_5 (m^3/m^3)	0.270	0.322	0.294	0.289	0.450	0.342	0.355	0.448	0.386	0.332	0.406	0.320
	SMC_{10} (m^3/m^3)	0.323	0.393	0.356	0.356	0.528	0.399	0.382	0.567	0.415	0.300	0.421	0.363
	ST_5 (°C)	16.3	22.6	19.6	7.5	18.4	14.1	8.1	16.3	14.1	12.1	20.7	16.9
	ST_{10} (°C)	14.2	22.8	18.8	4.2	17.1	11.6	4.3	15.8	9.6	9.9	20.2	15.2
	WT (cm)	-2.6	-24.8	-17.1	1.9	-15.8	-8.5	2.5	-15.9	-6.9	-0.4	-24.2	-12.9
N-ea	SMC_5 (m^3/m^3)	0.264	0.306	0.284	0.280	0.408	0.322	0.332	0.406	0.357	0.250	0.376	0.304
	SMC_{10} (m^3/m^3)	0.318	0.410	0.361	0.362	0.589	0.419	0.396	0.641	0.439	0.287	0.448	0.371
	ST_5 (°C)	14.1	20.5	17.5	5.2	16.2	11.8	5.7	14.1	11.8	9.8	18.5	14.7
	ST_{10} (°C)	12.1	20.3	16.5	3.5	14.9	9.8	3.6	13.6	7.9	8.2	17.9	13.1
	WT (cm)	-8.9	-31.1	-23.4	-3.5	-22.1	-14.7	-2.7	-22.2	-13.1	-6.6	-30.4	-19.2

In addition, annual records of ST_5 showed significant differences among the study sites (H = 66.4; p < 0.0001). However, pairwise comparisons revealed no significant difference between H-ea and L-ea (p = 0.564), but significant differences were observed between these two sites and N-ea (p < 0.0001). This condition may be associated with the higher vegetation cover at N-ea, which likely absorbed more solar radiation, thereby reducing direct soil heating. The annual mean ST_5 was 15.5 ± 4.6, 15.6 ± 3.6, and

https://doi.org/10.5194/egusphere-2025-3190
Preprint. Discussion started: 23 July 2025

13.4 ± 3.5 °C for H-ea, L-ea, and N-ea, respectively (Fig. S3). At the seasonal level, the Kruskal–Wallis test indicated significant differences among sites within each season (summer: $H = 126.9$; $p < 0.0001$; autumn: $H = 27.2$; $p < 0.0001$; winter: $H = 49.8$; $p < 0.0001$; spring: $H = 42.1$; $p < 0.0001$). Soil temperature at 10 cm depth (ST_{10}) also showed significant differences among the three sites ($H = 91.9$; $p < 0.0001$), with annual mean values of 14.8 ± 3.3, 13.7 ± 4.4, and 11.8 ± 4.1 °C for H-ea, L-ea, and N-ea, respectively (Fig. S4). Significant differences among sites were also observed across all seasons (summer: $H = 78.1$; $p < 0.0001$; autumn: $H = 46.1$; $p < 0.0001$; winter: $H = 112.5$; $p < 0.0001$; spring: $H = 42.8$; $p < 0.0001$). For both variables, the highest annual values were recorded during the first third of January 2022 at all three sites. This peak was associated with higher daily average solar radiation during that period (368.7 W m^{-2}), combined with low soil moisture content (Fig. S1 and S2). In addition, ST_{10} showed elevated values at the beginning of summer. Conversely, the lowest annual ST_5 and ST_{10} values were recorded between the last days of May and early June, due to low average air temperatures (three-day mean = 1.4 °C) and subzero minimum temperatures (three-day mean = −3.3 °C), which caused morning ground frosts. Seasonally, the highest mean values for both temperature variables across all sites were recorded in summer, and the lowest in winter (Table 1).

Annual WT data also showed significant differences among sites ($H = 227.3$; $p < 0.0001$), with H-ea exhibiting the highest levels (i.e., WT closer to or above the peat surface) and N-ea the lowest. The annual mean WT depth at each site was −9.6 ± 5.5 cm (H-ea), −11.3 ± 6.8 cm (L-ea), and −17.6 ± 6.8 cm (N-ea) (Fig. 3). Seasonal WT data also revealed significant differences among the three sites in every season (summer: $H = 80.4$; $p < 0.0001$; autumn: $H = 106.3$; $p < 0.0001$; winter: $H = 84.1$; $p < 0.0001$; spring: $H = 61.5$; $p < 0.0001$). All three sites recorded their highest WT levels in early July, associated with 70 mm of cumulative rainfall over the preceding three days. This led to localized flooding in parts of H-ea and L-ea, with water levels surpassing the peat surface. Conversely, the deepest WT levels were recorded at all sites in early February, following a 10-day period without precipitation. Across the study sites, the shallowest

https://doi.org/10.5194/egusphere-2025-3190
Preprint. Discussion started: 23 July 2025

seasonal WT levels (i.e., closest to the surface) were observed during winter, and the deepest during summer (Table 1).

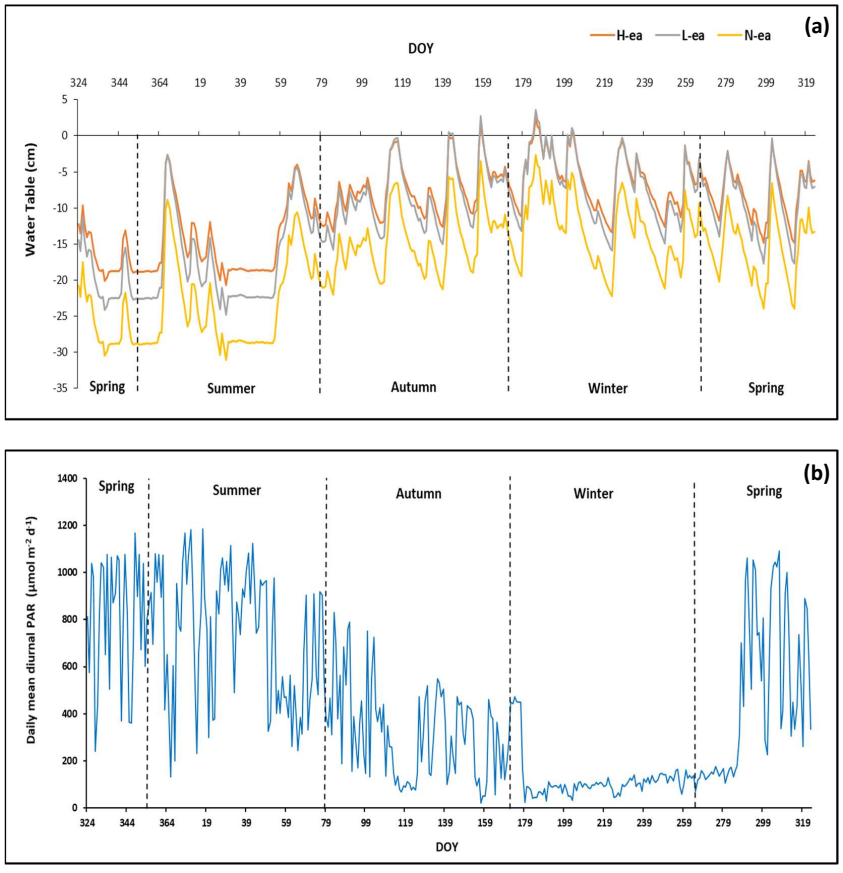

Figure 3. (a) Mean daily water table level at the three sites during the study period; (b) mean daily photosynthetically active radiation during the study period.

Daytime mean PAR values (i.e., PAR ≥ 20 µmol m^{-2} s^{-1}) recorded over the annual period averaged 433.8 ± 341.8 µmol m^{-2} s^{-1}. The highest PAR values were reached in mid January, with an average of 1178.2 ± 7.2 µmol m^{-2} s^{-1}, while the lowest readings were recorded between late June and early July, with

https://doi.org/10.5194/egusphere-2025-3190
Preprint. Discussion started: 23 July 2025

an average of 31.6 ± 7.1 µmol m^{-2} s^{-1} (Fig. 3). Seasonal average daily PAR values were 727.2 ± 279.2, 311.1 ± 195.4, 126.7 ± 93.4, and 584.4 ± 353.2 µmol m^{-2} s^{-1} for summer, autumn, winter, and spring, respectively. The lowest daily average PAR values for each season occurred in early January (summer), early June (autumn), late June (winter), and early in the season during spring. Conversely, the highest daily average PAR values were recorded in mid January (summer), late March (autumn), mid June (winter), and mid December (spring).

3.3. Annual and seasonal CO_2 fluxes

The model used to estimate GPP fluxes showed a good fit across the three study sites, with R^2 values of 0.94, 0.96, and 0.98, and RMSE values of 0.55, 0.57, and 0.43 for H-ea, L-ea, and N-ea, respectively, indicating a strong correspondence between observed and modeled data (Fig. S5). A similar pattern was observed in the R_{eco} modeling, with R^2 values of 0.88, 0.87, and 0.95, and RMSE values of 0.56, 0.46, and 0.49 for H-ea, L-ea, and N-ea, respectively (Fig. S6). The specific model parameters for GPP (α and GPP_{max}) and R_{eco} (R_{ref} and E_o) are reported by campaign and site in Tables S1–S3.

When considering integrated GPP fluxes over the annual period, the Kruskal–Wallis test revealed significant differences among sites ($H = 21.1$; $p < 0.0001$) (Fig. 4). During the study period, the highest mean daily GPP was recorded at N-ea with a value of −9.6 ± 5.9 g CO_2-C m^{-2} d^{-1} (most negative value), followed by L-ea (−8.6 ± 4.1) and H-ea (−6.8 ± 2.6 g CO_2-C m^{-2} d^{-1}). The highest daily average GPP rates at all three sites occurred in mid January (DOY 11), associated with high PAR levels. Additional GPP peaks were also observed in early December at H-ea and N-ea, and in late November at L-ea. The lowest mean daily GPP rates were recorded in early June (DOY 157), mid July (DOY 191), and mid June (DOY 171) for H-ea, L-ea, and N-ea, respectively (Fig. 5). Total accumulated GPP fluxes during the study period were −2490.1, −3159.1, and −3538.2 g CO_2-C m^{-2} for H-ea, L-ea, and N-ea, respectively. At the seasonal scale, the highest average daily GPP was recorded in summer for H-ea and N-ea (−8.9 ± 2.3 and −16.6 ± 2.5 g CO_2-C m^{-2} d^{-1}, respectively), and in spring for L-ea (−12.3 ± 2.4 g CO_2-C m^{-2} d^{-1}). Conversely, the lowest seasonal daily GPP

https://doi.org/10.5194/egusphere-2025-3190
Preprint. Discussion started: 23 July 2025

values occurred in winter at H-ea and N-ea (−4.7 ± 0.7 and −4.3 ± 0.6 g CO_2-C m^{-2} d^{-1}, respectively), and in autumn at L-ea (−5.3 ± 2.1 g CO_2-C m^{-2} d^{-1}) (Fig. 6). Compared to summer, winter GPP decreased by 47%, 52%, and 74% at H-ea, L-ea, and N-ea, respectively. The highest seasonal GPP accumulation occurred in spring at H-ea (−800.5 g CO_2-C m^{-2}) and L-ea (−1121.1 g CO_2-C m^{-2}), accounting for 32% and 35% of their respective annual totals. At N-ea, the greatest GPP accumulation was recorded in summer (−1497.1 g CO_2-C m^{-2}), representing 42% of the annual total. The lowest seasonal GPP accumulation occurred in winter for H-ea (−430.8 g CO_2-C m^{-2}) and N-ea (−394.5 g CO_2-C m^{-2}), corresponding to 17% and 11% of their respective annual GPP. In L-ea, the lowest accumulation was observed in autumn (−485.6 g CO_2-C m^{-2}), which represented 14% of the site's annual GPP. Overall, seasonal comparisons of average daily GPP showed minor differences between autumn and winter at L-ea, and between spring and summer at H-ea. In contrast, N-ea exhibited marked differences among all seasons.

https://doi.org/10.5194/egusphere-2025-3190
Preprint. Discussion started: 23 July 2025

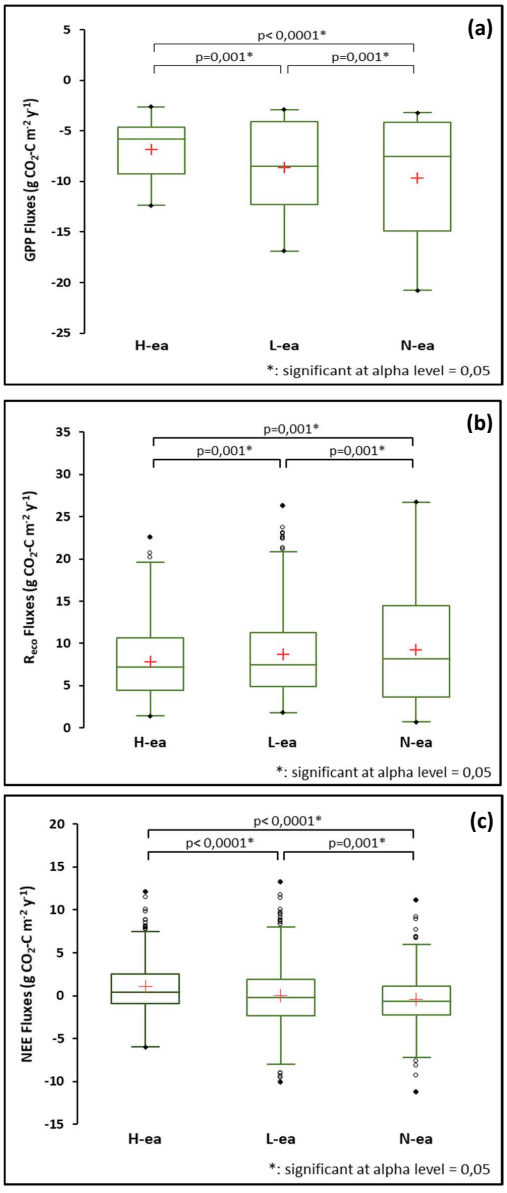

Figure 4. Boxplots of GPP (a), R_{eco} (b), and NEE (c) fluxes for each site. (Red crosses indicate mean values. Central horizontal bars represent medians. The lower and upper box edges correspond to the first and third quartiles, respectively. Black dots at the ends of the whiskers indicate the minimum and maximum values at each site. Points above or below the whisker limits may be considered outliers.)

https://doi.org/10.5194/egusphere-2025-3190
Preprint. Discussion started: 23 July 2025

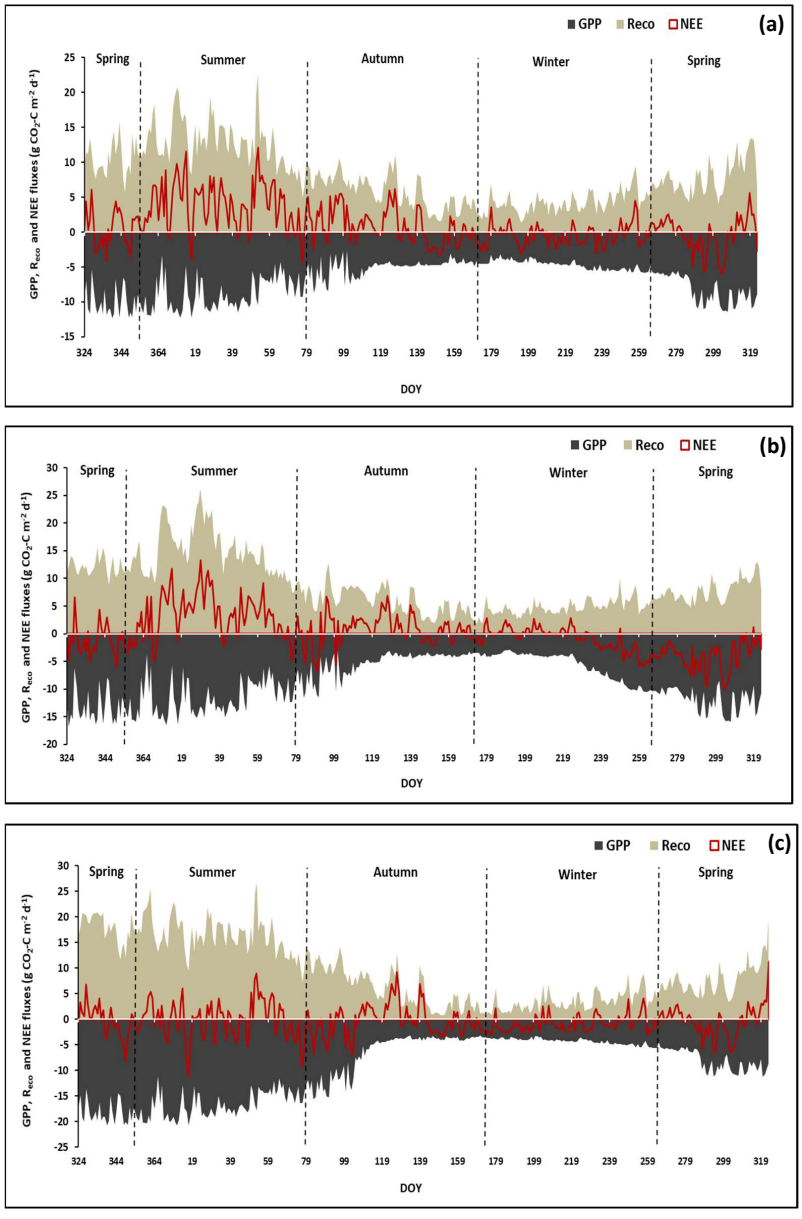

Figure 5. Annual dynamics of GPP, R_{eco}, and NEE fluxes (g CO_2-C m^{-2} d^{-1}) at H-ea (a), L-ea (b), and N-ea (c).

https://doi.org/10.5194/egusphere-2025-3190
Preprint. Discussion started: 23 July 2025

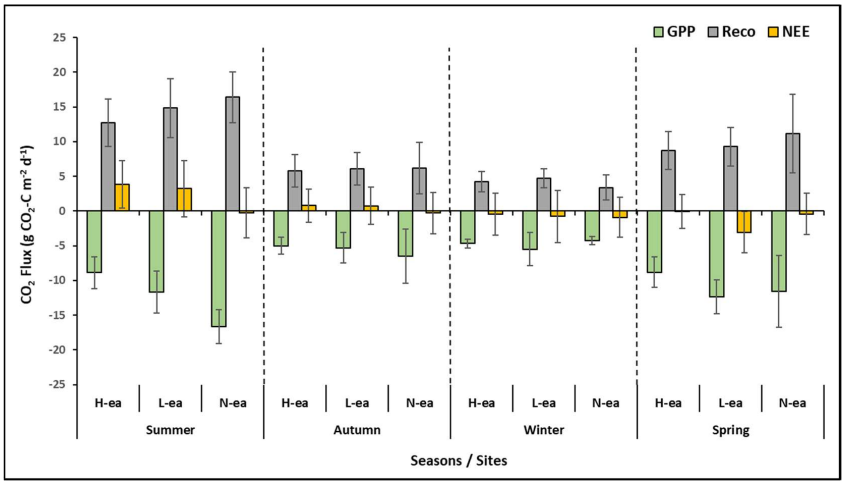

Figure 6. Seasonal GPP, R_{eco}, and NEE fluxes at the three study sites.

For annual integrated R_{eco} fluxes, the Kruskal–Wallis test revealed significant differences among sites (H = 200.7; p = 0.001) (Fig. 4). The highest daily mean R_{eco} fluxes were recorded in late February at H-ea and N-ea (DOY 53), and in late January at L-ea (DOY 29). An additional prominent peak occurred in mid January at H-ea and L-ea, and in late December at N-ea. Conversely, the lowest daily mean fluxes were observed in mid July at H-ea (DOY 195), and in late June at L-ea and N-ea (DOY 174) (Fig. 5). Over the full study period, the highest average daily R_{eco} was recorded at N-ea (9.2 ± 6.3 g CO_2-C m^{-2} d^{-1}), followed by L-ea (8.6 ± 4.8) and H-ea (7.8 ± 4.1) (Fig. 4). Total annual accumulated R_{eco} fluxes were 2865.7, 3169.2, and 3371.1 g CO_2-C m^{-2} for H-ea, L-ea, and N-ea, respectively. At the seasonal scale, the highest and lowest average daily R_{eco} values across all sites were recorded in summer (H-ea: 12.7 ± 3.4; L-ea: 14.9 ± 4.2; N-ea: 16.4 ± 3.7 g CO_2-C m^{-2} d^{-1}) and in winter (H-ea: 4.2 ± 1.5; L-ea: 4.7 ± 1.4; N-ea: 3.4 ± 1.8 g CO_2-C m^{-2} d^{-1}), respectively (Fig. 6). Compared to summer, average daily R_{eco} in winter decreased by 66%, 68%, and 79% at H-ea, L-ea, and N-ea, respectively. Among all seasons, winter showed the lowest accumulated R_{eco} at all three sites (H-ea: 389.2; L-ea: 433.8; N-ea: 312.2 g CO_2-C m^{-2}), accounting for 13%, 14%, and 9% of the

https://doi.org/10.5194/egusphere-2025-3190
Preprint. Discussion started: 23 July 2025

total annual R_{eco}, respectively. In contrast, summer recorded the highest seasonal R_{eco} fluxes (H-ea: 1145.9; L-ea: 1336.4; N-ea: 1475.7 g CO_2-C m^{-2}), representing 40%, 42%, and 44% of the respective annual totals. Seasonal comparisons of daily average values showed marked differences between seasons at all three sites.

Results for annual integrated NEE fluxes also showed significant differences among sites (H = 390.4; p < 0.0001) (Fig. 4). The annual average daily NEE values were 1.03 ± 3.04, 0.03 ± 0.19, and −0.46 ± 2.91 g CO_2-C m^{-2} d^{-1} for H-ea, L-ea, and N-ea, respectively. Corresponding annual accumulated NEE fluxes were 375.6, 10.2, and −167.1 g CO_2-C m^{-2}, indicating that only N-ea functioned as a net CO_2 sink. L-ea was near neutral, and H-ea acted as a net CO_2 source to the atmosphere (Fig. 7). Our results indicate that H-ea, L-ea, and N-ea acted as CO_2 sinks for 150, 194, and 214 days of the year, respectively. The peak daily CO_2 emission at each site occurred in late February at H-ea (DOY 53), late January at L-ea (DOY 29), and mid November at N-ea (DOY 323). Conversely, the highest daily uptake (most negative NEE) was recorded in late October at H-ea and L-ea (DOY 304), and in mid January at N-ea (DOY 17), indicating distinct seasonal patterns influenced by vegetation cover and composition (Fig. 5). At the seasonal level, the highest average daily emissions occurred during summer at H-ea and L-ea, with values of 3.8 ± 3.4 and 3.2 ± 4.1 g CO_2-C m^{-2} d^{-1}, respectively. In contrast, N-ea acted as a CO_2 sink throughout all four seasons. Notably, all three sites functioned as CO_2 sinks during spring and winter; however, H-ea showed only a weak sink behavior during spring. When comparing seasonal daily average NEE values, only N-ea exhibited consistent magnitudes and behavior (emission or sink) between summer and autumn.

https://doi.org/10.5194/egusphere-2025-3190
Preprint. Discussion started: 23 July 2025

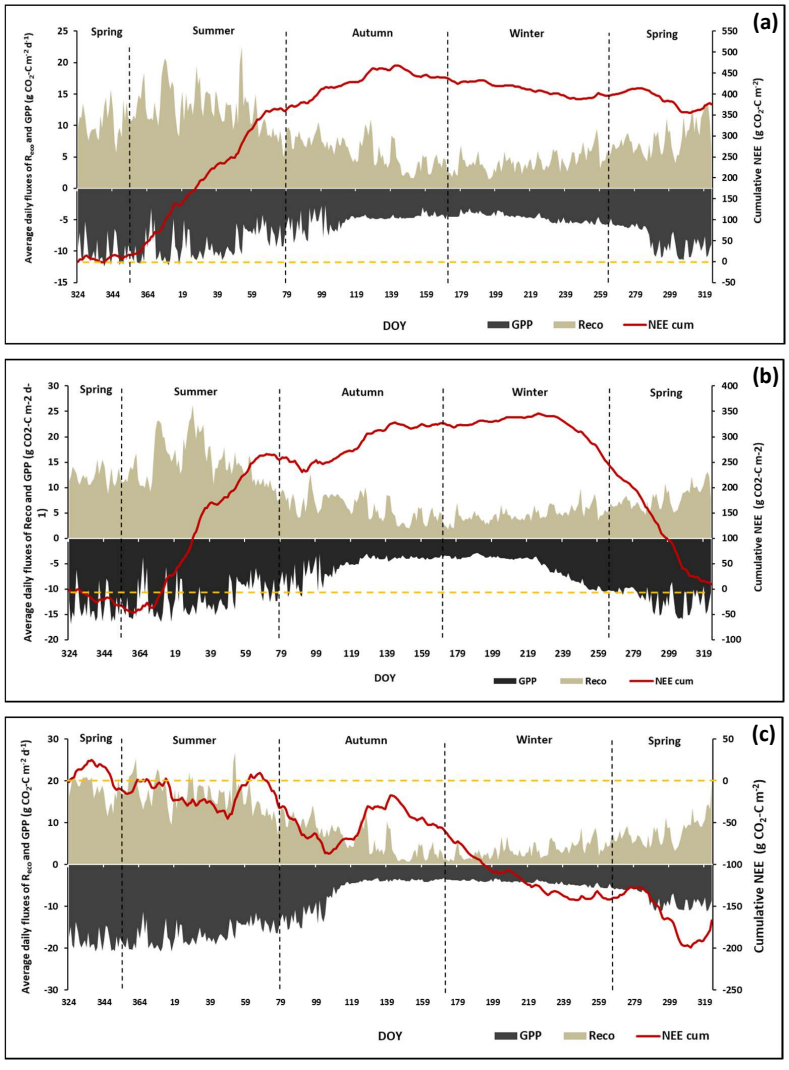

Figure 7. Cumulative NEE fluxes (solid red line) for H-ea (a), L-ea (b), and N-ea (c). The horizontal yellow dashed line indicates the zero level of the secondary axis corresponding to cumulative fluxes

https://doi.org/10.5194/egusphere-2025-3190
Preprint. Discussion started: 23 July 2025

3.4. Influence of environmental drivers on annual CO_2 fluxes

The results of the partial least squares regression (PLS-R) analysis for GPP across the different sites indicated a good model fit for H-ea and L-ea, with R^2 values of 0.73 and 0.77, respectively. In contrast, the model for N-ea showed a lower fit, with an R^2 value of 0.54. The PLS-R analysis identified PAR, T_{air}, ST_{10} and ST_5 as the most relevant drivers of GPP across all three sites. At H-ea and L-ea, only PAR surpassed the VIP threshold of 1, indicating a clearly dominant influence on GPP over the other environmental variables. At N-ea, both PAR and the temperature related variables (T_{air}, ST_{10}, and ST_5) exceeded the VIP = 1 threshold, indicating that they were the most influential on GPP at that site (Fig. 8).

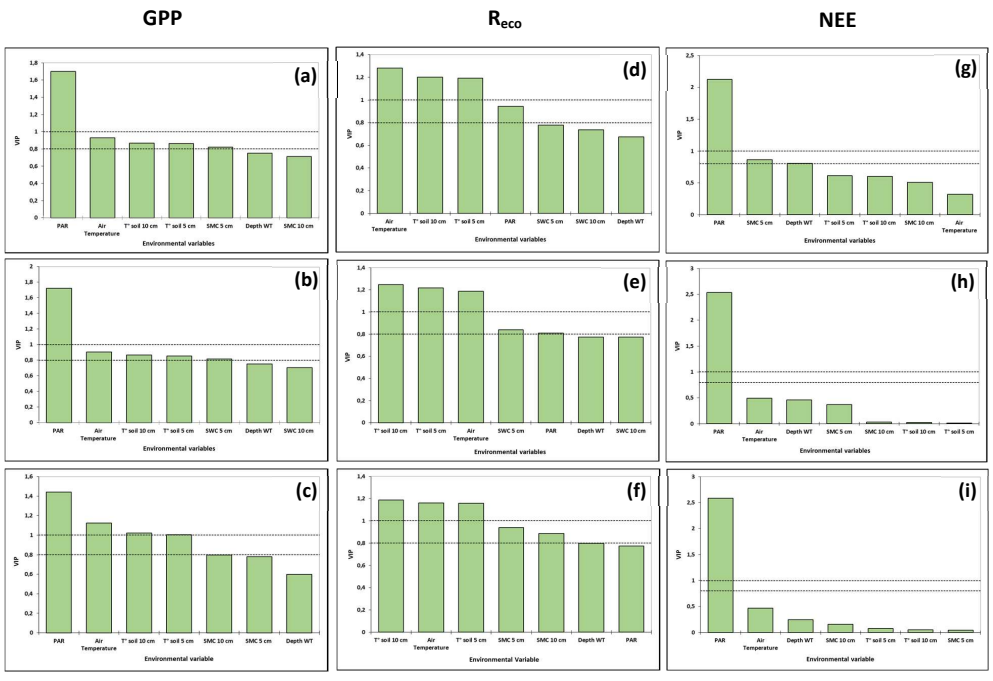

Figure 8. Variable importance in projection (VIP) scores obtained through partial least squares regression between GPP (a, b, c); R_{eco} (d, e, f); NEE (g, h, i) fluxes and different environmental drivers. Panels (a), (d), and (g) correspond to fluxes from H-ea; (b), (e), and (h) to fluxes from L-ea; and (c), (f), and (i) to fluxes from N-ea.

https://doi.org/10.5194/egusphere-2025-3190
Preprint. Discussion started: 23 July 2025

For R_{eco}, the regression models showed good fit at all three sites, with R^2 values of 0.76, 0.75, and 0.85 for H-ea, L-ea, and N-ea, respectively. The PLS-R analysis identified temperature related environmental variables, either T_{air} or soil temperatures (ST_{10} and ST_5), as the most influential for R_{eco} fluxes at all sites. ST_{10} was the predominant variable for R_{eco} at L-ea and N-ea, where both ST_5 and T_{air} also exceeded the VIP = 1 threshold. At H-ea, the most influential variable was T_{air}, although both ST_5 and ST_{10} also surpassed the VIP = 1 threshold. In addition to temperature, PAR and SMC_5 were also relevant variables for R_{eco} at the sites (VIP > 0.8) (Fig. 8).

Finally, the PLS-R models for NEE showed the weakest fits, with R^2 values of 0.32, 0.49, and 0.33 for H-ea, L-ea, and N-ea, respectively. The models clearly identified PAR as the dominant variable influencing NEE fluxes across all three sites, with VIP scores exceeding 1. At H-ea, both SMC_5 and WT were also considered important, with VIP scores above 0.8. In contrast, at L-ea and N-ea, no other variable exceeded a VIP of 0.5, indicating a predominant influence of PAR on NEE fluxes at those two sites (Fig. 8).

4. Discussion

4.1. Annual CO_2 flux dynamics

Analysis of the components of annual CO_2 fluxes revealed that both accumulated GPP and R_{eco} exhibited high magnitudes across the three study sites. Although such high rates are not commonly reported in the literature, studies on CO_2 fluxes in temperate warm peatlands in both hemispheres have yielded comparable results (Campbell et al., 2014; Beyer & Höper, 2015; Valdés-Barrera et al., 2019; D'Angelo et al., 2021; Gunawardhana et al., 2025), supporting our findings. Furthermore, the only previous study addressing annual CO_2 fluxes in an anthropogenic peatland of northern Patagonia subject to commercial *Sphagnum* harvesting (Valdés-Barrera et al., 2019) reported annual cumulative values for GPP and R_{eco} of 3599 ± 88 and 3567 ± 67 g CO_2 m^{-2}, respectively, similar to those observed in our study. The high annual GPP and R_{eco} rates in this geographic region are likely associated with environmental variables such as elevated PAR levels, warmer annual mean temperatures, longer photoperiods, and an extended growing

https://doi.org/10.5194/egusphere-2025-3190
Preprint. Discussion started: 23 July 2025

season (Frolking et al., 1998; Loisel et al., 2012; Helfter et al., 2015; Peichl et al., 2018). Additionally, our study area receives substantial annual precipitation, favoring soil moisture conditions throughout much of the year. In combination with these environmental factors, the presence of *Sphagnum* dominated vegetation and perennial vascular plants, especially shrubs and trees with higher leaf area indices, helps maintain year-round productivity. Similar patterns have been reported for peatlands in Australasia (Campbell et al., 2014; Gunawardhana et al., 2025). The annual cumulative NEE for the undisturbed site (N-ea), −167.1 g CO_2-C m^{-2}, falls within the range of values reported for other undisturbed temperate peatlands (Lafleur et al., 2001; Campbell et al., 2014; Helfter et al., 2015; Goodrich et al., 2017; Valdés-Barrera et al., 2019).

Significant differences in annual GPP were observed among sites (Fig. 4), with N-ea showing the highest mean daily GPP (−9.6 ± 5.9 g CO_2-C m^{-2} d^{-1}), which was 1.4 and 1.1 times higher than values recorded at H-ea and L-ea, respectively. This result can be attributed to a higher proportion of photosynthetically active biomass associated with dense vascular vegetation cover, particularly juvenile and more developed tree species, as well as small shrubs, both of which exhibit high leaf area indices and are composed entirely of perennial species. Additionally, a continuous *Sphagnum* moss layer covered the soil surface at N-ea, enhancing photosynthetic capacity (Korrensalo et al., 2016; Peichl et al., 2018; Kokkonen et al., 2022; Hanson et al., 2025). Peichl et al. (2018) suggested that the coexistence and balanced proportion of *Sphagnum* and vascular plant biomass are relevant to GPP in *Sphagnum* dominated peatlands. A lower average WT at N-ea, particularly during the growing season, may have enhanced vascular plant productivity (Sulman et al., 2010; Zhong et al., 2020), though it may also have reduced *Sphagnum* productivity (Helbig et al., 2022; Kokkonen et al., 2024). Conversely, the reduced *Sphagnum* cover at H-ea, resulting from commercial harvesting, and the unintended removal of vascular plants during repeated moss extraction using hooks and forks (Oberpaur et al., 2018), impaired photosynthetic performance. H-ea showed the lowest diversity of plant functional types, which likely limited its GPP (Ward et al., 2009; Kuiper et al., 2014; Laine et al., 2022). In addition, the open site conditions at H-ea, lacking protective

https://doi.org/10.5194/egusphere-2025-3190
Preprint. Discussion started: 23 July 2025

vascular vegetation, may have compromised *Sphagnum* photosynthetic efficiency, especially during the growing season (Hájek et al., 2009; Kokkonen et al., 2022).

In contrast, L-ea exhibited the presence of tree and shrub species, which likely facilitated *Sphagnum* establishment and productivity by providing protective cover against desiccation. Furthermore, the less intensive harvesting approach at L-ea allowed the site to maintain GPP levels close to those observed at the undisturbed area, demonstrating that maintaining ≥ 50% residual moss cover can contribute positively to productivity in the short term after harvesting (Pacheco-Cancino et al., 2023). Several studies have shown that in *Sphagnum* dominated peatlands, mosses play a key role in regulating GPP and the ecosystem C cycle. Despite having lower photosynthetic capacity than vascular plants, they contribute the majority of green biomass (Kuiper et al., 2014; Korrensalo et al., 2016; Voigt et al., 2024).

In peatland ecosystems, several studies have indicated that R_{eco} dynamics are primarily governed by thermal and hydrological regimes (Lafleur et al., 2005; Juszczak et al., 2013; Liu et al., 2024). However, it has also been noted that R_{eco} rates may be linked to vegetation photosynthetic activity and the subsequent release of root exudates that stimulate microbial decomposition of peat (Bubier et al., 2003; Basiliko et al., 2012; Bragazza et al., 2015; Korrensalo et al., 2020). Based on these insights, we can hypothesize that differences in R_{eco} fluxes among study sites (Fig. 4) may be associated with such drivers. R_{eco} dynamics were likely influenced by the soil thermal regime (ST_5 and ST_{10}), particularly during the growing season, a pattern consistent with findings from northern hemisphere temperate peatlands (Updegraff et al., 2001; Lafleur et al., 2005; Juszczak et al., 2013). Nevertheless, the lower soil temperature averages (ST_5 and ST_{10}) observed at N-ea would have been expected to reduce R_{eco} by limiting microbial activity, but this was not the case. On the contrary, N-ea exhibited the highest R_{eco} rates during the study period, which is inconsistent with the typically reported effects of soil temperature on R_{eco}. Differences in R_{eco} among sites may instead be linked to WT behavior. In this case, the higher respiration rates observed at N-ea may have been associated with a consistently deeper WT throughout the year (Fig. 3), which likely promoted aerobic decomposition of organic matter (Strack et al., 2014; Wilson et al., 2016; Górecki et al., 2021). Conversely,

https://doi.org/10.5194/egusphere-2025-3190
Preprint. Discussion started: 23 July 2025

shallower WT levels at H-ea and L-ea may have helped to reduce annual R_{eco} rates. Thus, at N-ea, the WT may have been a stronger driver of R_{eco} than the soil thermal regime, a condition also experimentally supported by previous studies (Munir et al., 2015; Pearson et al., 2015; Laine et al., 2019). Additionally, higher photosynthetic rates at N-ea, associated with greater biomass of *Sphagnum* and vascular plants, may have enhanced microbial activity and R_{eco} through the release of root exudates. In this regard, Crow & Wieder (2005) reported that vascular plants can contribute between 35% and 57% of the total surface peat respiration, mainly through rhizosphere processes, including root respiration and microbial mineralization of root exudates. With regard to NEE, H-ea functioned as a strong annual CO_2 source (375.6 g CO_2-C m^{-2} yr^{-1}) (Fig. 7), as GPP was not sufficient to offset site level R_{eco}, especially during the growing season. This condition was driven by reduced *Sphagnum* cover due to intensive harvesting and lower vascular plant biomass (Kuiper et al., 2014). In contrast, L-ea approached CO_2 neutrality (10.2 g CO_2-C m^{-2} yr^{-1}) (Fig. 7), likely due to greater *Sphagnum* cover after harvesting and a higher proportion of herbaceous and small shrub species, which contributed to increased GPP. This suggests that maintaining >50% residual moss cover after harvest may help mitigate the impacts of this anthropogenic disturbance on annual CO_2 fluxes. Similar values have been reported by Valdés-Barrera et al. (2019) for a peatland in northern Chiloé Island subject to commercial moss harvesting and livestock grazing, with an annual NEE of −35 g CO_2-C m^{-2} yr^{-1}. Finally, N-ea acted as a significant CO_2 sink during the year (−167.1 g CO_2-C m^{-2} yr^{-1}) (Fig. 7), due to continuous *Sphagnum* cover and a high proportion of perennial arboreal and shrubby vascular vegetation, which supported increased GPP, particularly during the growing season, exceeding R_{eco} (Zhong et al., 2020). Similar values were reported by Valdés-Barrera et al. (2019) for a section of anthropogenic peatland that had remained undisturbed for more than 40 years (−135 g CO_2-C m^{-2} yr^{-1}). Likewise, studies in undisturbed temperate *Sphagnum* dominated peatlands in Australasia indicate these ecosystems act as significant net C sinks, with reported values of −292.5 g C m^{-2} yr^{-1} (Gunawardhana et al., 2025) and −234.3 g C m^{-2} yr^{-1} (Campbell et al., 2014). Previous research in Finland (Silvan et al., 2017; Karjalainen et al., 2025) also confirms that *Sphagnum* harvesting areas show a reduced CO_2 sink capacity compared to undisturbed areas. Therefore, maintaining continuous *Sphagnum* moss cover is essential for peatlands to sustain their

https://doi.org/10.5194/egusphere-2025-3190
Preprint. Discussion started: 23 July 2025

function as CO_2 sinks (Brown et al., 2017; Purre et al., 2019; Kasimir et al., 2021; Pacheco-Cancino et al., 2023).

4.2. Seasonal dynamics of ecosystem net exchange

Annual NEE fluxes exhibited characteristic seasonal variations, with substantial daily fluctuations at all three sites, particularly during summer and spring, moderate in autumn, and low during winter, except for the final weeks of that season at the L-ea site (Fig. 5). Similar patterns have been observed in other studies of temperate peatlands in the Southern Hemisphere (Gunawardhana et al., 2025).

Distinct patterns of CO_2 emission and uptake were observed across sites at the seasonal scale (Fig. 6). The highest CO_2 emissions occurred during summer at H-ea and L-ea, with mean daily fluxes of 3.8 ± 3.4 and 3.2 ± 4.1 g CO_2-C m^{-2} d^{-1}, respectively. This may be attributed to increased R_{eco} driven by enhanced microbial activity associated with elevated air and soil temperatures and declining water table levels (Chivers et al., 2009; Helfter et al., 2015; Ofiti et al., 2021; Nielsen et al., 2023). Additionally, at H-ea, approximately 20% of the area consisted of bare peat patches resulting from repeated intensive harvesting. Previous studies have indicated that bare peat surfaces tend to increase R_{eco} rates during warmer periods compared to vegetated areas, as direct exposure to the atmosphere accelerates organic matter oxidation and heterotrophic respiration (Waddington & Warner, 2001; Petrone et al., 2003; Purre et al., 2019). Furthermore, lower moss and vascular plant cover at H-ea and L-ea meant that photosynthetic activity was insufficient to offset R_{eco}, contrasting with the conditions at N-ea, as also noted in other studies (McNeil & Waddington, 2003; Waddington et al., 2010; Kuiper et al., 2014). During autumn, H-ea and L-ea remained CO_2 sources, though with lower average daily values than in summer (H-ea: 0.8 ± 2.4; L-ea: 0.7 ± 2.6 g CO_2-C m^{-2} d^{-1}), due to declining R_{eco} driven by cooler temperatures and reduced photosynthetic activity associated with decreased PAR (AminiTabrizi et al., 2022; Antala et al., 2022). In contrast, N-ea functioned as a CO_2 sink, a condition also reported for other undisturbed temperate peatlands (Campbell et al., 2014), likely because *Sphagnum* mosses remain important

https://doi.org/10.5194/egusphere-2025-3190
Preprint. Discussion started: 23 July 2025

photosynthesizers during early spring and late autumn, when PAR is low (Korrensalo et al., 2017). Surprisingly, all three sites acted as CO_2 sinks during winter, an uncommon observation in the literature, as most evidence on this season derives from boreal and subarctic peatlands in the Northern Hemisphere (Bubier et al., 1998; Alm et al., 1999; Aurela et al., 2001; Aurela et al., 2002; Bäckstrand et al., 2010). In those ecosystems, CO_2 emissions tend to be high due to the cessation of photosynthesis under persistent snow cover, frozen soils (temperatures < 0 °C), and the dormancy or senescence of vegetation under low PAR (Alm et al., 1999; Aurela et al., 2001; Bubier et al., 2002). Northern temperate peatlands have also shown low winter emissions (~11 μg CO_2 m^{-2} s^{-1}) (Lafleur et al., 2001; Lund et al., 2007). In contrast, meteorological conditions in our study area during winter (precipitation and temperature) were more favorable for the continued productivity of *Sphagnum* and vascular plants, albeit at lower rates (Küttim et al., 2019; Bengtsson et al., 2020). Küttim et al. (2019) noted that, under suitable conditions, moss productivity during winter can account for 5–10% of annual totals, depending more on meteorological conditions than on plant ecophysiology or microsite characteristics. In the North Patagonian winter, the temperate oceanic climate (mean daily air temperature = 5.9 °C, with few frost days), sufficient PAR for photosynthetic activity (mean = 126 μmol m^{-2} s^{-1}, with > 200 μmol m^{-2} s^{-1} recorded during 10% of daytime hours) (Haraguchi & Yamada, 2011), and high rainfall frequency and quantity (Krebs et al., 2016) likely supported winter productivity at all study sites. These factors suggest that *Sphagnum* may have continued to grow during winter, contributing to the CO_2 sink condition (Malmer et al., 2003; Chong et al., 2015), a phenomenon also reported for a warm temperate peatland in Georgia (Transcaucasus) with similar climatic conditions (Krebs et al., 2016). Moreover, the fact that all vascular plant species recorded at the three sites were perennials may have further supported GPP. Similar findings were reported by Campbell et al. (2014) for a temperate peatland in New Zealand. In addition, during winter, all three sites exhibited the shallowest WT levels, which likely reduced R_{eco} rates by limiting aerobic oxidation of organic matter. Finally, we acknowledge the possibility that the GPP model may have overestimated winter productivity, as it does not account for reduced photosynthetic efficiency during this period (Shaefer et al., 2012). During spring, all three sites acted as CO_2 sinks, a condition also documented in other temperate peatlands

https://doi.org/10.5194/egusphere-2025-3190
Preprint. Discussion started: 23 July 2025

in the Southern Hemisphere (Campbell et al., 2014; Gunawardhana et al., 2025). However, H-ea exhibited a very weak daily mean uptake (−0.05 ± 2.5 g CO_2-C m^{-2} d^{-1}) compared to L-ea (−3.1 ± 2.9), where the highest seasonal cumulative NEE of the year was recorded. An early onset of the growing season, facilitated by warmer air temperatures (Fig. 2), and greater moss, forbs, and shrub cover (compared to H-ea), may have extended the photosynthetic period and enhanced spring sink strength (Peichl et al., 2015; Antala et al., 2022).

4.3. Environmental drivers of annual CO_2 fluxes

The PLS-R models consistently identified PAR as the most influential variable for GPP across the three study sites (VIP > 1), followed by variables associated with air and soil thermal regimes (T_{air}, ST_{10}, and ST_5), in agreement with several studies conducted in temperate peatlands (Loisel et al., 2012; Järveoja et al., 2018; Purre et al., 2019; Carbognani et al., 2023). In the case of *Sphagnum* GPP, Loisel et al. (2012) found that PAR was the primary predictor of moss growth based on a global dataset, reporting low productivity rates in cold climates with short growing seasons and low light availability, consistent with earlier observations by Hayward & Clymo (1983). Other studies have also reported that temperature positively influences moss growth in late summer and autumn, particularly for *S. magellanicum*, the dominant species at our study sites (Krebs et al., 2016; Walker et al., 2017; Bengtsson et al., 2020). Moore et al. (2006) indicated that soil temperature, more so than air temperature, shows a strong correlation with increased GPP in temperate peatlands. Meanwhile, photosynthesis in vascular vegetation is strongly driven by PAR and either air or soil temperature in mid latitude peatlands, where both factors determine photosynthetic efficiency and ecosystem scale carbon balance (Frolking et al., 1998; Strack et al., 2006; Riutta et al., 2007).

For R_{eco}, the PLS-R model identified T_{air} and soil temperatures (ST_{10} and ST_5) as the main environmental drivers. Our results are consistent with previous studies that identified thermal regimes as the dominant environmental controls on temporal variation in R_{eco} in peatlands (Lafleur et al., 2005; Mäkiranta et al., 2009; Juszczak et al., 2012; Juszczak et al., 2013), as warmer temperatures stimulate microbial activity,

https://doi.org/10.5194/egusphere-2025-3190
Preprint. Discussion started: 23 July 2025

resulting in increased CO_2 emissions. Some studies have shown that temporal variation in R_{eco} is tightly linked to peat temperature at 5 cm depth, explaining up to 94% of daily variation in some cases (Juszczak et al., 2013). Additionally, research in southeastern U.S.A. peatlands found that soil respiration increases with temperature, peaking at 25 °C, and that respiration sensitivity to temperature (Q_{10}) tends to increase with greater mean annual water table depth (Swails et al., 2022), a pattern observed at the N-ea site. These findings highlight the importance of surface air and soil temperatures as key drivers of R_{eco} in temperate peatlands.

Finally, the PLS-R model identified PAR as the most influential driver of annual NEE at all three study sites (VIP > 1). Soil temperature and SMC_5 were ranked much lower, with VIP values < 0.5. Studies in boreal peatlands confirm that NEE responds significantly to variations in PAR, especially during the growing season (Bubier et al., 1998), as observed at N-ea. Similarly, in restored peatlands, increases in PAR have been shown to enhance daytime CO_2 uptake (D'Acunha et al., 2019). Helbig et al. (2022), in a study of 20 Northern Hemisphere peatlands, found that mean site level annual CO_2 uptake increased with higher mean incident radiation, highlighting light availability as an important control on annual NEE fluxes. PAR exerted a decisive influence at all three sites, as evidenced by high daily NEE variability during the growing season (November to April), when PAR levels peaked. In contrast, during winter and late autumn, NEE variability decreased due to the more uniform behavior of PAR.

5. Conclusions

Our study successfully quantified annual and seasonal CO_2 fluxes using closed chambers in a temperate peatland of northern Patagonia following commercial harvesting of *Sphagnum magellanicum* under different extraction intensities, and compared them to an undisturbed reference site.

The annual cumulative GPP and R_{eco} fluxes were high across all three study sites compared to those reported for temperate peatlands in the Northern Hemisphere. This condition was associated with environmental variables that support greater productivity of mosses and dominant perennial vascular

https://doi.org/10.5194/egusphere-2025-3190
Preprint. Discussion started: 23 July 2025

vegetation. The cumulative NEE fluxes measured at the undisturbed site fell within the range reported for intact temperate peatlands in the Southern Hemisphere.

The intensity of commercial *Sphagnum* harvesting was directly correlated with annual NEE fluxes: the high intensity extraction site acted as a strong CO_2 source, the moderate intensity site exhibited near neutrality, and the undisturbed site functioned as an annual net CO_2 sink.

Seasonal NEE fluxes showed significant daily variations at all three sites during summer and spring, which stabilized by late autumn and throughout winter. The strongest CO_2 source behavior at disturbed sites occurred during summer, while the largest sink activity was observed during spring. The undisturbed site consistently captured CO_2 year-round. During winter, all three sites acted as CO_2 sinks due to less restrictive meteorological conditions that favored productivity and minimized respiration losses.

Annual GPP and NEE fluxes were driven by PAR, while R_{eco} was primarily controlled by air and soil thermal regimes, indicating that whether a peatland acts as a CO_2 source or sink is mainly determined by vegetation composition and cover, and their interaction with bioclimatic variables that influence productivity.

Our study provides valuable insights to bridge existing knowledge gaps and advance the understanding of CO_2 flux dynamics associated with commercial *Sphagnum* harvesting in temperate peatlands of the Southern Hemisphere. Furthermore, our findings may inform new policy proposals related to the conservation and sustainable management of peatlands in northern Patagonia.

Data Availability. All data presented in this study will be available at the time of publication.

Supplement. The supplement related to this article is available online at https://doi.org/10.5281/zenodo.15787948

https://doi.org/10.5194/egusphere-2025-3190
Preprint. Discussion started: 23 July 2025

Author contributions. **PP:** Writing – review & editing, Writing – original draft, Methodology, Investigation, Formal analysis. **RC:** Writing – review & editing, Investigation, Funding acquisition. **JR:** Writing – review & editing, Investigation. **MS:** Writing – review & editing, Resources, Funding acquisition.

Competing interests. The contact author has declared that none of the authors has any competing interests.

Acknowledgements. The authors are grateful for the funding granted by the Research Department of the Universidad de La Frontera, through the research project DIUFRO DI21-0096, to the Agencia Nacional de Investigacion y Desarrollo de Chile (ANID) for the funding granted through the National Doctoral Scholarship Folio No. 21191559, and to Mr. Héctor Aburto Olavarría for the facilities and collaboration provided to carry out this study on his property.

Funding information. DIUFRO Project DI21-0096, granted by the Research Department of the Universidad de La Frontera, Temuco, Chile. National Doctoral Scholarship No. 21191559, granted by Agencia Nacional de Investigación y Desarrollo de Chile (ANID).

https://doi.org/10.5194/egusphere-2025-3190
Preprint. Discussion started: 23 July 2025

References

Alm, J., Saarnio, S., Nykänen, H., Silvola, J., & Martikainen, P. J.: Winter CO_2, CH_4 and N_2O fluxes on some natural and drained boreal peatlands. *Biogeochemistry*, 44, 163-186. https://doi.org/10.1007/BF00992977, 1999.

AminiTabrizi, R., Dontsova, K., Graf Grachet, N., & Tfaily, M. M.: Elevated temperatures drive abiotic and biotic degradation of organic matter in a peat bog under oxic conditions. *Science of the Total Environment*, 804, 150045. https://doi.org/10.1016/j.scitotenv.2021.150045, 2012.

Antala, M., Juszczak, R., van der Tol, C., & Rastogi, A.: Impact of climate change-induced alterations in peatland vegetation phenology and composition on carbon balance. *Science of the Total Environment*, 827, 154294. https://doi.org/10.1016/j.scitotenv.2022.154294, 2022.

Aurela, M., Laurila, T., & Tuovinen, J-P.: Seasonal CO_2 balance of a subartic mire. *Journal of Geophysical Research,* 106, 1623-1637. https://doi.org/10.1029/2000JD900481, 2001.

Aurela, M., Laurila, T., & Tuovinen, J-P.: Annual CO_2 balance of a subarctic fen in northern Europe: Importance of the wintertime efflux. *Journal of Geophysical Research*, 107, 4607. https://doi.org/10.1029/2002JD002055, 2002.

Bäckstrand, K., Crill, P. M., Jackowicz-Korczynski, M., Mastepanov, M., Christensen, T. R., & Bastviken, D.: Annual carbon gas budget for a subarctic peatland, Northern Sweden. *Biogeosciences*, 7, 95-108. https://doi.org/10.5194/bg-7-95-2010, 2010.

Baird, A. J., Green, S. M., Brown, E., Dooling, G. P.: Modelling time-integrated fluxes of CO_2 and CH_4 in peatlands: a review. *Mires and Peat*, 24, 1–15. https://doi.org/10.19189/MaP.2019.DW.395., 2019

Basiliko, N., Stewart, H., Roulet, N. T., Moore, T.: Do root exudates enhance peat decomposition? *Geomicrobiol J.*, 29 (4), 374–378. https://doi.org/10.1080/01490451.2011.568272, 2012.

https://doi.org/10.5194/egusphere-2025-3190
Preprint. Discussion started: 23 July 2025

795 Bayer, A., Bachmann, M., Müller, A., Kaufmann, H.: A comparison of feature-based MLR and PLS regression
796 techniques for the prediction of three soil constituents in a degraded south African ecosystem. *Appl.*
797 *Environ. Soil Sci.*, 971252. https://doi.org/10.1155/2012/971252, 2012.

798 Beetz, S., Liebersbach, H., Glatzel, S., Jurasinski, G., Buczko, U., Höper, H.: Effects of land use intensity on
799 the full greenhouse gas balance in an Atlantic peat bog. *Biogeosciences*, 10(2), 1067–1082.
800 https://doi.org/10.5194/bg-10-1067-2013, 2013.

801 Bengtsson, F., Rydin, H., Baltzer, J., Bragazza, L., Bu, Z-J., Caporn, S. J. M., Dorrepaal, E., Flatberg, K. I.,
802 Galanina, O., Gałka, M., Ganeva, A., Goia, I., Goncharova, N., Hájek, M., Haraguchi, A., Harris, L.,
803 Humphreys, E., Jiroušek, M., Kajukało, K., Karofeld, E.,…& Granath, G.: Environmental drivers of *Sphagnum*
804 growth in peatlands across the Holarctic región. *Journal of Ecology*, 109, 417-431.
805 https://doi.org/10.1111/1365-2745.13499, 2020

806 Beyer, C., & Höper, H.: Greenhouse gas exchange of rewetted bog peat extraction and a *Sphagnum*
807 cultivation site in Northwest Germany. *Biogeosciences*, 12, 2101–2117. https://doi.org/10.5194/bg-12-
808 2101-2015, 2015.

809 Blodau, C.: Carbon cycling in peatlands – a review of processes and control. *Environ. Rev.*, 10, 111-134.
810 https://doi.org/10.1139/a02-004, 2002.

811 Blok, C., Eveleens, B., & van Winkel, A.: Growing media for food and quality of life in the period 2020-2050.
812 *Acta Horticulturae*, 1305, 341-355. https://doi.org/10.17660/ActaHortic.2021.1305.46, 2021.

813 Bragazza, L., Bardgett, R. D., Mitchell, E. A., Buttler, A.: Linking soil microbial communities to vascular plant
814 abundance along a climate gradient. *New Phytol.*, 205, 1175–1182. https://doi.org/10.1111/nph.13116,
815 2015.

https://doi.org/10.5194/egusphere-2025-3190
Preprint. Discussion started: 23 July 2025

816 Brown, C., Strack, M., & Price, J. S.: The effects of water management on the CO_2 uptake of *Sphagnum*
817 moss in a reclaimed peatland. *Mires and Peat*, *20*(5), 1–15. http://mires-and-
818 peat.net/media/map20/map_20_05.Pdf, 2017.

819 Bubier, J., Crill, P. M., Moore, T. R., Savage, K., & Varner, R. K.: Seasonal patterns and controls on net
820 ecosystem CO_2 exchange in a boreal peatland complex. *Global Biogeochemical Cycles*, 12, 4, 703-714.
821 https://doi.org/10.1029/98GB02426, 1998.

822 Bubier, J., Crill, P., Mosedale, A., Frolking, S., & Linder, E.: Peatland responses to varying interannual
823 moisture conditions as measured by automatic CO_2 chambers. *Global Biogeochemical Cycles*, 17, 2, 1066.
824 https://doi.org/0.1029/2002GB001946, 2003.

825 Campbell, D. I., Smith, J., Goodrich, J. P., Wall, A. M., & Schipper, L. A.: Year-round growing conditions
826 explains large CO_2 sink strength in a New Zealand raised peat bog. *Agricultural and Forest Meteorology*,
827 192-193, 59-68. https://doi.org/10.1016/j.agrformet.2014.03.003, 2014.

828 Carbognani, M., Tomaselli, M., Petraglia, A.: Interactions and covariation of ecological drivers control CO_2
829 fluxes in an alpine peatland. *Wetlands,* 43, 44. https://doi.org/10.1007/s13157-023-01692-5, 2023.

830 Carrasco, M., Dec, D., Valle, S. R., Zúniga, F., Dörner, J.: Historial de uso de un suelo ñadi: consecuencias
831 sobre la capacidad efectiva de almacenamiento de agua/ aire y la continuidad del medio poroso (historical
832 use of a Ñadi soil: consequences on the effective capacity to storage water/air and the continuity of the
833 pore system). *Rev. Agro Sur,* 45 (1), 39–51. https://doi.org/10.4206/agrosur.2017.v45n1-06., 2017.

834 Chivers, M. R., Turetsky, M. R., Waddington, J. M., Harden, J. W., & McGuire, A. D.: Effects of Experimental
835 Water Table and Temperature Manipulations on Ecosystem CO_2 Fluxes in an Alaskan Rich Fen. *Ecosystem*,
836 12, 1329-1342. https://doi.org/0.1007/s10021-009-9292-y, 2009.

https://doi.org/10.5194/egusphere-2025-3190
Preprint. Discussion started: 23 July 2025

837 Chong, M., Humphreys, E., and Moore, T. R.: Microclimatic response to increasing shrub cover and its
838 effect on *Sphagnum* CO_2 exchange in a bog. *Écoscience*, 19 (1), 89–97. https://doi:10.2980/19-1-3489.,
839 2015.

840 Crown, S. E., & Wieder, R. K.: Sources of CO_2 emission from a northern peatland: root respiration,
841 exudation, and decomposition. *Ecology*, 86 (7), 1825-1834. https://doi.org/10.1890/04-1575, 2005.

842 D'Acunha, H., Sonnentag, O., Humphreys, E. R., & Basiliko, N.: Net ecosystem carbon balance of a peat bog
843 undergoing restoration: Integrating CO_2 and CH_4 fluxes from eddy covariance and aquatic evasion with
844 DOC drainage fluxes. *Journal of Geophysical Research: Biogeosciences*, 124(12), 3725–3742.
845 https://doi.org/10.1029/2019JG005123, 2019.

846 D'Angelo, B., Leroy, F., Guimbaud, C., Jacotot, A., Zocatelli, R., Gogo, S., & Laggoun-Défarge, F.: Carbon
847 balance and spatial variability of CO_2 and CH_4 fluxes in a *Sphagnum*-dominated peatland in a temperate
848 climate. *Wetlands*, *41*, 5. https://doi.org/10.1007/s13157-021-01411-y, 2021.

849 Díaz, M. F., Larraín, J., Zegers, G., & Tapia, C.: Caracterización florística e hidrológica de turberas de la Isla
850 Grande de Chiloé, Chile. *Rev. Chilena de Hist. Nat.*, 81, 445–68. https://doi.org/10.4067/S0716-
851 078X2008000400002, 2008.

852 Díaz, M. F., Tapia, C., Jiménez, P., Bacigalupe, L.: *Sphagnum magellanicum* growth and productivity in
853 Chilean anthropogenic peatlands. *Rev. Chil. Hist. Nat*. 85, 513–518. https://doi.org/10.4067/S0716-
854 078X2012000400013, 2012.

855 Díaz, M. F., & Silva, W.: Antecedentes generales sobre las turberas en el sur de Chile. Cap 1: 15-32, En:
856 Turberas de *Sphagnum* de Chiloé, ¿Como hacer un uso sustentable?, editado por: Oberpaur, C., Díaz, M.
857 F. y León, C. 1ra edición. Ediciones Universidad Santo Tomás. Santiago, Chile. 120 pp., 2018.

https://doi.org/10.5194/egusphere-2025-3190
Preprint. Discussion started: 23 July 2025

Di Castri, F., & Hajek, E. R.: Bioclimatología de Chile. Vicerrectoría Académica Universidad Católica de Chile, Santiago, Chile, 159 pp., 1976.

Dickopp, J., Lengerer, A., & Kazda, M.: Relationship between groundwater levels and oxygen availability in fen peat soils. *Ecological Engineering*, 120, 85-93. https://doi.org/10.1016/j.ecoleng.2018.05.033, 2018.

Dunn, C. & Freeman, C.: Peatlands: our greatest source of carbon credits?. *Carbon Management*, 2(3), 289–301. https://doi.org/10.4155/cmt.11.23, 2011.

Eickenscheidt, T., Heinichen, J., Drösler, M.: The greenhouse gas balance of a drained fen peatland is mainly controlled by land-use rather than soil organic carbon content. *Biogeosciences* 12, 5164–5184. https://doi.org/10.5194/bg-12-5161-2015, 2015.

Elsgaard, L., Görres, C. M., Hoffmann, C. C., Blicher-Mathiesen, G., Schelde, K., Petersen, S. O.: Net ecosystem exchange of CO_2 and carbon balance for eight temperate organic soils under agricultural management. *Agric. Ecosyst. Environ.*, 162, 52–67. https://doi.org/10.1016/j.agee.2012.09.001, 2012.

Finlayson, C. M., Milton, G. R.: Peatlands. In: Finlayson, C., Milton, G., Prentice, R., Davidson, N. (eds.) The Wetland Book. Springer, Dordrecht. https://doi.org/10.1007/978-94-007-6173-5_202-1, 2016.

Frolking, S. E., Bubier, J. L., Moore, T. R., Ball, T., Bellisario, L. M., Bhardwaj, A., Carroll, P., Crill, P. M., Lafleur, P. M., McCaughey, J. H., Roulet, N. T., Suyker, A. E., Verma, S. B., Waddington, J. M., Whiting, G. J.: Relationship between ecosystem productivity and photosynthetically active radiation for northern peatlands. *Global Biochem. Cycles*, 12 (1), 115–126. https://doi.org/10.1029/97GB03367, 1998.

Frolking, S., Talbot, J., Jones, M. C., Treat, C. C., Kauffman, J. B., Tuittila, E-S., & Roulet, N.: Peatlands in the Earth's 21st century climate system. *Environmental Reviews*, 19, 371-396. https://doi.org/10.1139/a11-014, 2011.

https://doi.org/10.5194/egusphere-2025-3190
Preprint. Discussion started: 23 July 2025

879 Goodrich, J. P., Campbell, D. I., & Schipper, L. A.: Southern Hemisphere bog persists as a strong carbon sink
880 during droughts. *Biogeosciences*, 14, 4563-4576. https://doi.org/10.5194/bg-14-4563-2017, 2017.

881 Górecki, K., Rastogi, A., Stróżecki, M., Gąbka, M., Lamentowicz, M., Łuców, D., Kayzer, D., & Juszczak, R.:
882 Water table depth, experimental warming, and reduced precipitation impact on litter decomposition in a
883 temperate *Sphagnum*-peatland. *Science of the Total Environment*, 771, 145452.
884 https://doi.org/10.1016/j.scitotenv.2021.145452, 2021.

885 Gunawardhana, M., Treby, S., Silvester, E., Callesen, T. O., Jones, O. A. H., & Grover, S.: Intact Australian
886 *Sphagnum* peatland is a strong carbon sink. *Science of the Total Environment*, 959, 178197.
887 https://doi.org/10.1016/j.scitotenv.2024.178197, 2025.

888 Hájek, T., Tuittila, E-S., Ilomets, M., & Laiho, R.: Light responses of mire mosses – a key to survival after
889 water-level drawdown?. *Oikos*, 118**,** 240–250. https://doi.org/10.1111/j.1600-0706.2008.16528.x, 2009.

890 Hanson, P. J., Griffiths, N. A., Salmon, V. G., Birkebak, J. M., Warren, J. M., Phillips, J. R., Guilliams, M. P.,
891 Oleheiser, K. C., Jones, M. W., Jones, N. J., Enterkine, J., Glenn, N. F., & Pearson, K. J.: Peatland plant
892 community changes in annual production and composition through 8-years of warming manipulations
893 under ambient and elevated CO_2 atmospheres. *Journal of Geophysical Research: Biogeosciences*, *130*,
894 e2024JG008511. https://doi.org/10. 1029/2024JG008511, 2025.

895 Haraguchi, A. & Yamada, N.: Temperature Dependency of Photosynthesis of *Sphagnum* spp. Distributed in
896 the Warm-Temperate and the Cool-Temperate Mires of Japan. *American Journal of Plant Sciences*, 2, 716-
897 725. https://doi.org/10.4236/ajps.2011.25086, 2011.

898 Harenda, K. M., Lamentowicz, M., Samson, M., Chojnicki, B. H.: The Role of Peatlands and Their Carbon
899 Storage Function in the Context of Climate Change. In: Zielinski, T., Sagan, I., Surosz, W. (eds.)
900 Interdisciplinary Approaches for Sustainable Development Goals. GeoPlanet: Earth and Planetary Sciences.
901 Springer, Cham. https://doi.org/10.1007/978-3-319-71788-3_12, 2018.

https://doi.org/10.5194/egusphere-2025-3190
Preprint. Discussion started: 23 July 2025

902 Harris, L., Richardson, K., Bona, K. A., Davidson, S. J., Finkelstein, S. A., Garneau, M., McLaughlin, J., Nwaishi,
903 F., Olefeldt, D., Packalen, M., Roulet, N. T., Southee, F. M., Strack, M., Webster, K. L., Wilkinson, S. L., &
904 Ray, J. C.: The essential carbon service provided by northern peatlands. *Frontiers in Ecology and the*
905 *Environment*, 20, 4, 222-230. https://doi.org/10.1002/fee.2437, 2022.

906 Hayward, P. M., & Clymo, R. S.: The growth of *Sphagnum*: Experiments on, and simulation of, some effects
907 of light flux and water-table depth. *Journal of Ecology*, 71(3), 845–863. https://doi.org/10.2307/2259597,
908 1983.

909 Heinemeyer, A., McNamara, N. P.: Comparing the closed static versus the closed dynamic chamber flux
910 methodology: implications for soil respiration studies. *Plant Soil,* 346, 145–151.
911 https://doi.org/10.1007/s11104-011-0804-0, 2011.

912 Heinemeyer, A., Asena, Q., Lee Burn, W., Lloyd Jones, A.: Peatland carbon stocks and burn history: blanket
913 bog peat core evidence highlights charcoal impacts on peat physical properties and long-term carbon
914 storage. *Geo Geogr. Environ.*, 6, 1, e00063. https://doi.org/10.1002/geo2.63, 2018.

915 Helbig, M., Živković, T., Alekseychik, P., Aurela, M., El-Madany, T. S., Euskirchen, E. S., Flanagan, L. B.,
916 Griffis, T. J., Hanson, P. J., Hattakka, J., Helfter, C., Hirano, T., Humphreys, E. R., Kiely, G., Kolka, R., Laurila,
917 T., Leahy, P. G., Lohila, A., Mammarella, I., Nilsson, M. B., Panov, A., Parmentier, F. J. W., Peichl, M., Rinne,
918 J., Roman, D., Sonnentag, O.,Tuittila, E-S., Ueyama, M., Vesala, T., Vestin, P., Weldon, S., Weslien, P., &
919 Zaehle, S.: Warming response of peatland CO_2 sink is sensitive to seasonality in warming trends. *Nat. Clim.*
920 *Chang,* 12, 743–749. https://doi.org/10.1038/s41558-022-01428-z, 2022.

921 Helfter, C., Campbell, C., Dinsmore, K. J., Drewer, J., Coyle, M., Anderson, M., Skiba, U., Nemitz, E, Billett,
922 M. F., & Sutton, M. A.: Drivers of long-term variability in CO_2 net ecosystem exchange in a temperate
923 peatland. *Biogeosciences*, 12, 1799-1811. https://doi.org/10.5194/bg-12-1799-2015, 2015.

https://doi.org/10.5194/egusphere-2025-3190
Preprint. Discussion started: 23 July 2025

924 Järveoja, J., Peichl, M., Maddison, M., Soosaar, K., Vellak, K., Karofeld, E., Teemusk, A., Mander, U.: Impact
925 of water table level on annual carbon and greenhouse gas balances of a restored peat extraction area.
926 *Biogeosciences*, 13, 2637–2651. https://doi.org/10.5194/bg-13-2637-2016, 2016.

927 Järveoja, J., Nilsson, M. B., Gazovic, M., Crill, P. M., Peichl, M.: Partitioning of the net CO_2 exchange using
928 an automated chamber system reveals plant phenology as key control of production and respiration fluxes
929 in a boreal peatland. *Glob. Chang. Biol.*, 24, 3436–3451. https://doi.org/10.1111/gcb.14292, 2018.

930 Johnson, K. A., Godoy, R. S.: The original Michaelis constant: translation of the 1913 Michaelis-Menten
931 paper. *Biochemistry* 50, 8264–8269. https://doi.org/10.1021/bi201284u, 2011.

932 Joosten, H., Sirin, A., Couwenberg, J., Laine, J. & Smith, P.: The role of peatlands in climate regulation. In
933 Bonn, A., Joosten, H., Evans, M., Stoneman, R., & Allott, T. (eds.) Peatland Restoration and Ecosystem
934 Services: Science, Policy and Practice Ecological Reviews. Cambridge: University Press, pp 63–76.
935 https://doi.org/10.1017/CBO9781139177788.005, 2016.

936 Juszczak, R., Acosta, M., Olejnik, J.: Comparison of daytime and nighttime ecosystem respiration measured
937 by the closed chamber technique on temperate mire in Poland. *Pol. Journal Environ Stud.*, 21(3), 643–658.,
938 2012.

939 Juszczak, R., Humphreys, E., Acosta, M., Michalak-Galczewska, M., Kayser, D., Olejnik, J.: Ecosystem
940 respiration in a heterogeneous temperate peatland and its sensitivity to peat temperature and water table
941 depth. *Plant Soil,* 366, 505–520. https://doi.org/10.1007/s11104-012-1441-y, 2013.

942 Karjalainen, S. K., Anttila, J., Maanavilja, L., Hamedianfar, A., Laine, A. M.: Carbon dioxide and methane gas
943 exchange following *sphagnum* moss harvesting in boreal peatland. J. *Environ. Manag.* 373, 123357.
944 https://doi.org/10.1016/j.jenvman.2024.123357, 2025.

https://doi.org/10.5194/egusphere-2025-3190
Preprint. Discussion started: 23 July 2025

945 Kasimir, A., He, H., Jansson, P.-E., Lohila, A., & Minkkinen, K.: Mosses are important for soil carbon
946 sequestration in forested peatlands. *Frontiers in Environmental Science*, *9*, 680430.
947 https://doi.org/10.3389/fenvs.2021.680430, 2021.

948 Kelly, J., Kljun, N., Eklunndh, L., Klemedtsson, L., Liljebladh, B., Olsson, P-O., Weslien, P., & Xie, X.: Modelling
949 and upscaling ecosystem respiration using thermal cameras and UAVs: application to a peatland during
950 and after a hot drought. *Agri. Forestr. Meteorol.*, 300, 108330. doi:
951 https://doi.org/10.1016/j.agrformet.2021.108330, 2021.

952 Kokkonen, N., Laine, A. M., Männistö, E., Mehtätalo, L., Korrensalo, A., & Tuittila, E-S.: Two Mechanisms
953 Drive Changes in Boreal Peatland Photosynthesis Following Long-Term Water Level Drawdown: Species
954 Turnover and Altered Photosynthetic Capacity. *Ecosystem*, 25, 1601-1618.
955 https://doi.org/10.1007/s10021-021-00736-3, 2022.

956 Kokkonen, N., Laine, A. M., Korrensalo, A., Nijp, J., Limpens, J., Mehtätalo, L., Männistö, E., & Tuittila, E-S.:
957 A deepened water table increases the vulnerability of peat mosses to periodic drought. *Journal of Ecology*,
958 112, 1210-1224. https://doi.org/10.1111/1365-2745.14305, 2024.

959 Korrensalo, A., Hájek, T., Vesala, T., Mehtätalo, L., & Tuittila, E-S.: Variation in photosynthetic properties
960 among bog plants. *Botany*, 94, 1127-1139. https://doi.org/10.1139/cjb-2016-0117, 2016.

961 Korrensalo, A., Alekseychik, P., Hájek, T., Rinne, J., Vesala, T., Mehtätalo, L., Mammarella, I., & Tuitila, E-S.:
962 Species-specific temporal variation in photosynthesis as a moderator of peatland carbon sequestration.
963 *Biogeosciences*, 14, 257–269. https://doi.org/10.5194/bg-14-257-2017, 2017.

964 Korrensalo, A., Mehtätalo, L., Alekseychik, P., Uljas, S., Mammarella, I., Vesala, T., Tuittila, E.-S.: Varying
965 vegetation composition, respiration and photosynthesis decrease temporal variability of the CO_2 sink in a
966 boreal bog. *Ecosystem*, 23, 842–858. https://doi.org/10.1007/s10021-019-00434-1, 2020.

https://doi.org/10.5194/egusphere-2025-3190
Preprint. Discussion started: 23 July 2025

967 Kuiper, J. J., Mooij, W. M., Bragazza, L., and Robroek, B. J.: Plant functional types define magnitude of
968 drought response in peatland CO_2 exchange. *Ecology*, 95(1), 123–131. https://doi.org/10.1890/13-027.1,
969 2014.

970 Küttim, M., Küttim, L., Ilomets, M., & Laine, A. M.: Controls of *Sphagnum* growth and the role of Winter.
971 *Ecological Research*, 35, 219-234. https://doi.org/10.1111/1440-1703.12074, 2019.

972 Krebs, M., Gaudig, G., & Joosten H.: Record growth of *Sphagnum papillosum* in Georgia (Transcaucasus):
973 rain frequency, temperature and microhabitat as key drivers in natural bogs. *Mires and Peat*, 4, 1-16.
974 https://doi.org/10.19189/MaP.2015.OMB.190, 2016.

975 Lafleur, P. M., Roulet, N. T. & Admiral, S. W.: Annual cycle of CO_2 exchange at a bog peatland. *J. Geophys.*
976 *Res.-Atmos.* 106, 3071–3082. https://doi.org/10.1029/2000JD900588, 2001.

977 Lafleur, P. M., Moore, T. R., Roulet, N. T., & Frolking, S.: Ecosystem respiration in a cool temperate bog
978 depends on peat temperature but not water table. *Ecosystems*, 8, 619–629.
979 https://doi.org/10.1007/s10021-003-0131-2, 2005.

980 Laine, A. M., Wilson, D., Alm, J., Schneider, J., Tuittila, E.-S.: Spatial variation in potential photosynthesis in
981 northern European bogs. *J. Veg. Sci.*, 27 (2), 365–376. https://doi.org/10.1111/jvs.12355, 2016.

982 Laine, A. M., Mehtälalo, L., Tolvanen, A., Frolking, S., & Tuittila, E-S.: Impacts of drainage, restoration and
983 warming on boreal wetland greenhouse gas fluxes. *Science of the Total Environment*, 647, 169-181.
984 https://doi.org/10.1016/j.scitotenv.2018.07.390, 2019.

985 Laine, A. M., Korrensalo, A., Tuittila, E-S.: Plant functional traits play the second fiddle to plant functional
986 types in explaining peatland CO_2 and CH_4 gas Exchange. *Science of the Total Environment*, 834, 155352.
987 https://doi.org/10.1016/j.scitotenv.2022.155352, 2022.

https://doi.org/10.5194/egusphere-2025-3190
Preprint. Discussion started: 23 July 2025

Leifeld, J., & Menichetti, L.: The underappreciated potential of peatlands in global climate change mitigation strategies. *Nat. Commun.*, 9, 1071. https://doi.org/10.1038/s41467-018-03406-6, 2018.

Leifeld, J., Wüst-Galley, C., & Page, S.: Intact and managed peatland soils as a source and sink of GHGs from 1850 to 2100. *Nat. Clim. Change.*, 9, 945-947. https://doi.org/10.1038/s41558-019-0615-5, 2019.

León, C., Oliván, G., & Fuertes, E.: Turberas esfagnosas de Chiloé (Chile) y su problemática ambiental. *Boletín de la Sociedad Española de Briología*, *38–39*, 29–40. https://biblioteca.cehum. org/handle/CEHUM 2018/1411, 2012.

León, C. A., Oliván Martínez, G., & Aurora, G.: Environmental Controls of Cryptogam Composition and Diversity in Anthropogenic and Natural Peatland Ecosystems of Chilean Patagonia. *Ecosystems,* 21, 203–215. https://doi.org/10.1007/s10021-017-0142-z, 2018.

León, C. A., Gabriel, M., Rodríguez, C., Iturraspe, R., Savoretti, A., Pancotto, V., Benítez-Mora, A., Valdés, A., Díaz, M. F., Oberpaur, C., Domínguez, E., Fernández, L. D., Mackenzie, R., Roland, T., Mauquoy, D., & Silva, C.: Peatlands of Southern South America: A review. *Mires and Peat*, *3*, 1–29. http://mires-and-peat.net/media/map27/map_27_03.Pdf, 2021.

Li, Y., Henrion, M., Moore, A., Lambot, S., Opfergelt, S., Vanacker, V., Jonard, F., Van Oost, K.: Factors controlling peat soil thickness and carbon storage in temperate peatlands based on UAV high-resolution remote sensing. *Geoderma*, 449, 117009. https://doi.org/10.1016/j.geoderma.2024.117009, 2024.

Limpens, J., Berendse, F., Blodau, C., Canadell, J. G., Freeman, C., Holden, J., Roulet, N., Rydin, H. & Schaepman-Strub, G.: Peatlands and the carbon cycle: from local processes to global implications–a synthesis. *Biogeosciences*, 5, 1475-1491. https://doi.org/10.5194/bg-5-1475-2008, 2008.

https://doi.org/10.5194/egusphere-2025-3190
Preprint. Discussion started: 23 July 2025

1008 Liu, H., Rezanezhad, F., Zhao, Y., He, H., Van Cappellen, P., & Lennartz, B.: The apparent temperature
1009 sensitivity (Q_{10}) of peat soil respiration: A synthesis study. *Geoderma*, 443, 116844.
1010 https://doi.org/10.1016/j.geoderma.2024.116844, 2024.

1011 Lloyd, J., & Taylor, J. A.: On the temperature dependence of soil respiration. *Funct. Ecol.*, 8, 315–323.
1012 https://doi.org/10.2307/2389824, 1994.

1013 Loisel, J., Gallego-Sala, A. V., & Yu, Z.: Global-scale pattern of peatland *Sphagnum* growth driven by
1014 photosynthetically active radiation and growing season length. *Biogeosciences*, *9*, 2737–2746.
1015 https://doi.org/10.5194/bg-9-2737-2012, 2012.

1016 Loisel, J., Gallego-Sala, A.: Ecological resilience of restored peatlands to climate change. *Commun. Earth*
1017 *Environ*., 3, 208. https://doi.org/10.1038/s43247-022-00547-x, 2022.

1018 Lopatin, J., Araya-López, R., Galleguillos, M., Perez-Quezada, J. F.: Disturbance alters relationships between
1019 soil carbon pools and aboveground vegetation attributes in an anthropogenic peatland in Patagonia. *Ecol.*
1020 *Evol.*, 12 (3), e8694. https://doi.org/10.1002/ece3.8694, 2022.

1021 Lund, M., Lindroth, A., Christensen, T. R., & Ström, L.: Annual CO_2 balance of a temperate bog. *Tellus*, 59B,
1022 804-811. https://doi.org/10.1111/j.1600-0889.2007.00303.x, 2007.

1023 Mäkiranta, P., Laiho, R., Fritze, H., Hytönen, J, Laine J, Minkkinen, K.: Indirect regulation of heterotrophic
1024 peat soil respiration by water level via microbial community structure and temperature sensitivity. *Soil*
1025 *Biol. Biochem*., 41, 695–703. https://doi.org/10.1016/j.soilbio.2009.01.004, 2009.

1026 Malmer, N., Albinsson, C., Svensson, B. M., Wallén, B.: Interferences between *Sphagnum* and vascular
1027 plants: effects on plant community structure and peat formation. *Oikos,* 100, 469–482.
1028 https://doi.org/10.1034/j.1600-0706.2003.12170.x, 2003.

https://doi.org/10.5194/egusphere-2025-3190
Preprint. Discussion started: 23 July 2025

1029 Martin, C. R., Zeng, N., Karion, A., Dickerson, R. R., Ren, X., Turpie, B. N., Weber, K. J.: Evaluation and
1030 environmental correction of ambient CO_2 measurements from a low-cost NDIR sensor. *Atmos. Meas.*
1031 *Tech.,* 10, 2383–2395. https://doi.org/10.5194/amt-10-2383-2017, 2017.

1032 Mattila, T. J.: The role of peatlands in carbon footprints of countries and products. *Science of the Total*
1033 *Environment,* 947, 174552. https://doi.org/10.1016/j.scitotenv.2024.174552, 2024.

1034 McNeil, P., & Waddington, J. M.: Moisture controls on *Sphagnum* growth and CO_2 exchange on a cutover
1035 bog. *Journal of Applied Ecology*, *40*, 354–367. https://www.jstor.org/stable/3506008, 2003.

1036 Mecagga, R., Asante, M., Sossa, G., Antonijevic, D., Dubbert, M., Hoffmann, M.: Validation and field
1037 application of a low-cost device to measure CO_2 and evapotranspiration (ET) fluxes. *Atmos. Meas. Tech.*,
1038 17, 1317–1332. https://doi.org/10.5194/amt-17-1317-2024, 2024.

1039 Michaelis, L., & Menten, M. L.: Die Kinetik der Invertinwirkung. *Biochem*. Z. 49, 333–369, 1913.

1040 Moore, T. R., Lafleur, P. M., Poon, D. M. I., Heumann, B. W., Seaquist, J. W., & Roulet, N. T.: Spring
1041 photosynthesis in a cool temperate bog. *Glob. Change Biol.,* 12 (12), 2323–2335.
1042 https://doi.org/10.1111/j.1365-2486.2006.01247.x, 2006.

1043 Munir, T. M., Perkins, M., Kaing, E., & Strack, M.: Carbon Dioxide Flux and Net Primary Production of a
1044 Boreal Treed Bog Responses to Warming and Water-table-lowering Simulations of Climate Change.
1045 *Biogeosciences,* 12 (4), 1091–1111. https://doi:10.5194/bg-12-1091-2015, 2015.

1046 Murray, K. R., Borkenhagen, A. K., Cooper, D. J., & Strack, M.: Growing season carbon gas exchange from
1047 peatlands used as a source of vegetation donor material for restoration. *Wetlands Ecology and*
1048 *Management*, *25*, 501–515. https://doi.org/10.1007/s11273-017-9531-5, 2017.

https://doi.org/10.5194/egusphere-2025-3190
Preprint. Discussion started: 23 July 2025

1049 Nielsen, C. K., Elsgaard, L., Jørgensen, U., & Laerke, P. E.: Soil greenhouse gas emissions from drained and
1050 rewetted agricultural bare peat mesocosms are linked to geochemistry. *Science of the Total Environment*,
1051 896, 165083. https://doi.org/10.1016/j.scitotenv.2023.165083, 2023.

1052 Oberpaur, C., Díaz, M. F., & Castillo, N.: Recolección sustentable de musgo *Sphagnum* en turberas y
1053 pomponales de la región de Los Lagos. Cap 3: 45-73. En: Turberas de *Sphagnum* de Chiloé, ¿Cómo hacer
1054 un uso sustentable?, editado por: Oberpaur, C., Díaz, M. F. y León, C. 1ra edición. Ediciones Universidad
1055 Santo Tomás. Santiago, Chile. 120 pp., 2018.

1056 Ofiti, N. O. E., Solly, E. F., Hanson, P. J., Malhotra, A., Wiesenberg, G. L. B., & Schmidt, M. W.: Warming and
1057 elevated CO_2 promote rapid incorporation and degradation of plant-derived organic matter in an
1058 ombrotrophic peatland. *Global Change Biology*, 28, 883–898. https://doi.org/10.1111/gcb.15955, 2021.

1059 Pacheco-Cancino, P. A., Carrillo-López, R. F., Sepulveda-Jauregui, A., & Somos-Valenzuela, M. A.:
1060 *Sphagnum* mosses, the impact of disturbances and anthropogenic management actions on their ecological
1061 role in CO_2 fluxes generated in peatland ecosystems. *Global Change Biology*, 00, e16972.
1062 https://doi.org/10.1111/gcb.16972, 2023.

1063 Pacheco-Cancino, P. A., Carrillo-López, R. F., Riquelme-Belmar, J. A., & Somos-Valenzuela, M. A.: Impacts
1064 of differents intensities of comercial *Sphagnum* moss extraction on CO_2 fluxes in a northern Patagonia
1065 peatland. *Science of the Total Environment*, 964, 178566.
1066 https://doi.org/10.1016/j.scitotenv.2025.178566, 2025.

1067 Pearson, M., T. Penttila, L. Harjunpaa, R. Laiho, J. Laine, T. Sarjala, K. Silvan, and N. Silvan.: Effects of
1068 Temperature Rise and Water-table-level Drawdown on Greenhouse Gas Fluxes of Boreal Sedge Fens.
1069 *Boreal Environment Research,* 20, 489–505. http://urn.fi/URN:NBN:fi-fe2016082623053, 2015.

1070 Peichl, M., Öquist, M., Ottosson Löfvenius, M., Ilstedt, U., Sagerfors, J., Grelle, A., Lindroth, A., Nilsson, M.
1071 B.: A 12 years record reveals pre-growing season temperature and water table level threshold effects on

https://doi.org/10.5194/egusphere-2025-3190
Preprint. Discussion started: 23 July 2025

1072 the net carbon dioxide exchange in a boreal fen. *Environ. Res. Lett*. 9, 055006.
1073 https://doi.org/10.1088/1748-9326/9/5/055006, 2014.

1074 Peichl, M., Sonnentag, O., Nilsson, M. B.: Bringing color into the picture: using digital repeat photography
1075 to investigate phenology controls of the carbon dioxide exchange in a boreal mire. *Ecosystems*, 18, 115–
1076 131. https://doi.org/10.1007/s10021-014-9815-z, 2015.

1077 Peichl, M., Gažovič, M., Vermeij, I., De Goede, E., Sonnentag, O., Limpens, J., Nilsson, M. B.: Peatland
1078 vegetation composition and phenology drive the seasonal trajectory of maximum gross primary
1079 production. *Sci. Rep*., 8, 1–11. https://doi.org/10.1038/s41598-018-26147-4, 2018.

1080 Pérez-Quezada, J. F., Moncada, M., Barrales, P., Urrutia-Jalabert, R., Pfeiffer, M., Farías Herrera, A., &
1081 Sagardía, R.: How much carbon is stored in the terrestrial ecosystems of the Chilean Patagonia?. *Austral*
1082 *Ecology*, 48, 5, 893-903. https://doi.org/10.1111/aec.13331, 2023.

1083 Petrone, R. M., Waddington, J. M., & Price, J. S.: Ecosystem-scale flux of CO_2 from a restored vacuum
1084 harvested peatland. *Wetlands Ecol. Manage*., 11, 419 – 432.
1085 https://doi.org/10.1023/B:WETL.0000007192.78408.62, 2003.

1086 Purre, A.-H., Pajula, R., & Ilomets, M.: Carbon dioxide sink function in restored milled peatlands—The
1087 significance of weather and vegetation. *Geoderma*, *346*, 30–42.
1088 https://doi.org/10.1016/j.geoderma.2019.03.032, 2019.

1089 Rankin, T., Roulet, N., Humphreys, E., Peichl, M., & Järveoja, J.: Partitioning autotrophic and heterotrophic
1090 respiration in an ombrotrophic bog. *Front. Earth Sci*., 11, 1263418.
1091 https://doi.org/10.3389/feart.2023.1263418, 2023.

1092 Riutta, T., Laine, J., & Tuittila, E. S.: Sensitivity of CO_2 exchange of fen ecosystem components to water
1093 level variation. *Ecosystems,* 10(5), 718–733. https://doi.org/10.1007/s10021-007-9051-3, 2007.

https://doi.org/10.5194/egusphere-2025-3190
Preprint. Discussion started: 23 July 2025

Saarnio, S., Morero, M., Shurpali, N. J., Tuittila, E-S., Mäkilä, M., & Alm J.: Annual CO_2 and CH_4 fluxes of pristine boreal mires as a background for the lifecycle analyses of peat energy. *Boreal Environment Research*, 12, 101-113. http://hdl.handle.net/10138/235361, 2007.

Samaritani, E., Siegenthaler, A., Yli-Petäys, M., Buttler, A., Christin, P-A., Mitchell, E. A. D.: Seasonal net ecosystem carbon exchange of a regenerating cutaway bog: how long does it take to restore the C-sequestration function?. *Restor. Ecol.*, 19 (4), 480–489. https://doi.org/10.1111/j.1526-100X.2010.00662.x, 2011.

Schaefer, K., Schwalm, C. R., Williams, C., Arain, M. A., Barr, A., Chen, J. M., Davis, K. J., Dimitrov, D., Hilton, T. W., Hollinger, D. Y., Humphreys, E., Poulter, B., Raczka, B. M., Ricahardson, A. D., Sahoo, A., Thornton, P., Vargas, R., Verbeeck, H., Anderson, R., Baker, I., …& Zhou, X.: A model-data comparison of gross primary productivity: Results from the North American Carbon Program site synthesis. *Journal of Geophysical Research*, 117, G03010. https://doi.org/10.1029/2012JG001960, 2012.

Silvan, N., Jokinen, K., Näkkilä, J., & Tahvonen, R.: Swift recovery of *Sphagnum* carpet and carbon sequestration after shallow *Sphagnum* biomass harvesting. *Mires and Peat*, *20*, 1–11. http://mires-and-peat.net/media/map20/map_20_01.pdf, 2017.

Sirin, A. A.: Mires and Peatlands: Carbon, Greenhouse Gases, and Climate Change. *Biol Bull Rev.*, 12 (Suppl 2), S123–S139. https://doi.org/10.1134/S2079086422080096, 2022.

Strack, M., Waddington, J. M., Tuittila, E. S., & Rochefort, L.: Response of vegetation and net ecosystem exchange at different peatland microforms following water table drawdown. *Journal of Geophysical Research: Biogeosciences*, 111, G02006. https://doi.org/10.1029/2005JG000145, 2006.

Strack, M., Keith, A. M., Xu, B.: Growing season carbon dioxide and methane exchange at a restored peatland on the Western boreal plain. *Ecol. Eng.*, 64, 231–239. https://doi.org/10.1016/j.ecoleng.2013.12.013, 2014.

https://doi.org/10.5194/egusphere-2025-3190
Preprint. Discussion started: 23 July 2025

1117 Strack, M., Davidson, S. J., Hirano, T., Dunn, C.: The Potential of Peatlands as Nature-Based Climate
1118 Solutions. *Curr. Clim. Change. Rep.,* 8, 71–82. https://doi.org/10.1007/s40641-022-00183-9, 2022.

1119 Sulman, B. N., Desai, A. R., Saliendra, N. Z., Lafleur, P. M., Flanagan, L. B., Sonnentag, O., Mackay, D. S.,
1120 Barr, A. G., van der Kamp, G.: CO_2 fluxes at northern fens and bogs have opposite responses to inter-annual
1121 fluctuations in water table. *Geophys. Res. Lett.*, 37, L19702, http://dx.doi.org/10.1029/2010gl044018,
1122 2010.

1123 Swails, E. E., Ardón, M., Krauss, K. W., Peralta, A. L., Emanuel, R. E., Helton, A. M., Morse, J. L., Gutenberg,
1124 L., Cormier, N., Shoch, D., Settlemyer, S., Soderholm, E., Boutin, B. P., Peoples, C., Ward, S.: Response of
1125 soil respiration to changes in soil temperature and water table level in drained and restored peatlands of
1126 the southeastern United States. *Carbon Bal. Manag.*, 17, 18. http://doi.org/10.1186/s13021-022-00219-
1127 5, 2022.

1128 UNEP: Global Peatlands Assessment – The State of the World's Peatlands: Evidence for action toward the
1129 conservation, restoration, and sustainable management of peatlands. Main Report. Global Peatlands
1130 Initiative. United Nations Environment Programme, Nairobi. 418 pp., 2022

1131 Updegraff, K., Bridgham, S., Pastor, J., Weishampel, P., Harth, C.: Response of CO_2 and CH_4 emissions from
1132 peatlands to warming and water table manipulation. *Ecol. Appl.*, 11 (2), 311–326.
1133 https://doi.org/10.2307/3060891, 2001.

1134 Valdés-Barrera, A., Kutzbach, L., Celis-Diez, J. L., Armesto, J. J., Holl, D., & Pérez-Quezada, J. F.: Effects of
1135 disturbance on the carbon dioxide balance of an anthropogenic peatland in Northern Patagonia. *Wetland*
1136 *Ecology Management*, *27*(5–6), 635–650. https://doi.org/10.1007/s11273-019-09682-3, 2019.

1137 Vega-Vilca, J. C., Guzmán, J.: Regresión PLS y PCA como solución al problema de multicolinealidad en
1138 regresión múltiple. *Rev. Matemática, Teoría y Aplic.*, 18 (1), 9–20.
1139 https://www.scielo.sa.cr/pdf/rmta/v18n1/a02v18n1.pdf, 2010.

https://doi.org/10.5194/egusphere-2025-3190
Preprint. Discussion started: 23 July 2025

1140 Viru, B., Veber, G., Jaagus, J., Kull, A., Maddison, M., Muhel, M., Espenberg, M., Teemusk, A., & Mander,
1141 Ü.: Wintertime Greenhouse Gas Fluxes in Hemiboreal Drained Peatlands. *Atmosphere*, 11, 7, 731.
1142 https://doi.org/10.3390/atmos11070731, 2020.

1143 Voigt, C., Dubbert, M., Launiainen, S., Porada, P., Oestmann, J., & Piayda, A.: Impact of vegetation
1144 composition and seasonality on sensitivity of modelled CO_2 exchange in temperate raised bogs. *Scientific*
1145 *Report*, 14, 11023. https://doi.org/10.1038/s41598-024-61229-6, 2024.

1146 Waddington, J. M., & Warner, K. D.: Atmospheric CO_2 sequestration in restored mined peatlands.
1147 *Ecoscience*, 8, 359 – 368. https://doi.org/10.1080/11956860.2001.11682664, 2001.

1148 Walker, A. P., Carter, K. R., Gu, L., Hanson, P. J., Malhotra, A., Norby, R. J., Sebestyen, S. D., Wallschleger,
1149 S. D., & Weston, D. J.: Biophysical drivers of seasonal variability in *Sphagnum* gross primary production in
1150 a northern temperate bog. *J. Geophys. Res. Biogeosci.*, 122, 1078–1097.
1151 https://doi.org/10.1002/2016JG003711, 2017.

1152 Ward, S. E., Bardgett, R. D., McNamara, N. P., & Ostle, N. J.: Plant functional group identity influences
1153 short-term peatland ecosystem carbon flux: Evidence from a plant removal experiment. *Functional*
1154 *Ecology*, *23*, 454–462. https://doi.org/10.1111/j.1365-2435.2008.01521.x, 2009.

1155 Whinam, J., & Buxton, R.: *Sphagnum* peatlands of Australasia: An assessment of harvesting sustainability.
1156 *Biological Conservation*, *82*, 21–29. https://doi.org/10.1016/S0006-3207(97)00015-3, 1997.

1157 Whinam, J., Hope, G. S., Clarkson, B. R., Buxton, R. P., Alspach, P. A., & Adam, P.: *Sphagnum* in peatlands
1158 of Australasia: Their distribution, utilisation and management. *Wetlands Ecology and Management*, *11*,
1159 37–49. https://doi.org/10.1023/A:1022005504855, 2003.

https://doi.org/10.5194/egusphere-2025-3190
Preprint. Discussion started: 23 July 2025

1160 Wilson, D., Farrell, C. A., Fallon, D., Moser, G., Müller, C., Renou-Wilson, F.: Multiyear greenhouse gas
1161 balances at a rewetted temperate peatland. *Glob. Chang. Biol.*, 22 (12), 4080–4095.
1162 https://doi.org/10.1111/gcb.13325, 2016.

1163 Wright, E. L., Black, C. R., Cheesman, A. W., Drage, T., Large, D., Turner, B. L., Sjögersten, S.: Contribution
1164 of subsurface peat to CO_2 and CH_4 fluxes in a neotropical peatland. *Glob. Chang. Biol.,* 17 (9), 2867–2881.
1165 https://doi.org/10.1111/j.1365-2486.2011.02448.x, 2011.

1166 Yu, Z., Loisel, J., Brosseau, D., Beilman, D., Hunt, S.: Global peatland dynamics since the last glacial
1167 maximum. *Geophys. Res. Lett.*, 37, L13402. https://doi.org/10.1029/2010GL043584, 2010.

1168 Yu, Z. C.: Northern peatland carbon stocks and dynamics: a review. *Biogeosciences*, 9, 4071–4085.
1169 https://doi.org/10.5194/bg-9-4071-2012, 2012.

1170 Zhong, Y., Jiang, M., & Middleton, B. A.: Effects of water level alteration on carbon cycling in peatlands.
1171 *Ecosystem Health and Sustainability*, 6, 1, 1806113. https://doi.org/10.1080/20964129.2020.1806113,
1172 2020.